



HAL
open science

New 8-Nitroquinolinone Derivative Displaying Submicromolar in Vitro Activities against Both *Trypanosoma brucei* and *cruzi*

Julien Pedron, Clotilde Boudot, Jean-Yves Brossas, Emilie Pinault, Sandra Bourgeade-Delmas, Alix Sournia-Saquet, Elisa Boutet-Robinet, Alexandre Destere, Antoine Tronnet, Justine Bergé, et al.

► To cite this version:

Julien Pedron, Clotilde Boudot, Jean-Yves Brossas, Emilie Pinault, Sandra Bourgeade-Delmas, et al.. New 8-Nitroquinolinone Derivative Displaying Submicromolar in Vitro Activities against Both *Trypanosoma brucei* and *cruzi*. ACS Medicinal Chemistry Letters, 2020, 11 (4), pp.464-472. 10.1021/ac-smedchemlett.9b00566 . hal-02476867

HAL Id: hal-02476867

<https://unilim.hal.science/hal-02476867>

Submitted on 15 May 2020

HAL is a multi-disciplinary open access archive for the deposit and dissemination of scientific research documents, whether they are published or not. The documents may come from teaching and research institutions in France or abroad, or from public or private research centers.

L'archive ouverte pluridisciplinaire **HAL**, est destinée au dépôt et à la diffusion de documents scientifiques de niveau recherche, publiés ou non, émanant des établissements d'enseignement et de recherche français ou étrangers, des laboratoires publics ou privés.



Distributed under a Creative Commons Attribution 4.0 International License

New 8-Nitroquinolinone Derivative Displaying Submicromolar *in Vitro* Activities against Both *Trypanosoma brucei* and *cruzi*

Julien Pedron,⁺ Clotilde Boudot,⁺ Jean-Yves Brossas, Emilie Pinault, Sandra Bourgeade-Delmas, Alix Sournia-Saquet, Elisa Boutet-Robinet, Alexandre Destere, Antoine Tronnet, Justine Bergé, Colin Bonduelle, Céline Deraeve, Geneviève Pratviel, Jean-Luc Stigliani, Luc Paris, Dominique Mazier, Sophie Corvaisier, Marc Since, Aurélie Malzert-Fréon, Susan Wyllie, Rachel Milne, Alan H. Fairlamb, Alexis Valentin, Bertrand Courtioux, and Pierre Verhaeghe*

Cite This: *ACS Med. Chem. Lett.* 2020, 11, 464–472

Read Online

ACCESS |

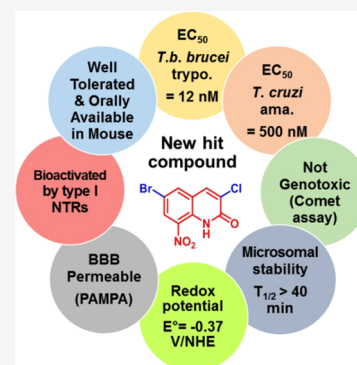
Metrics & More

Article Recommendations

Supporting Information

ABSTRACT: An antikinoplastid pharmacomodulation study was conducted at position 6 of the 8-nitroquinolin-2(1H)-one pharmacophore. Fifteen new derivatives were synthesized and evaluated *in vitro* against *L. infantum*, *T. brucei brucei*, and *T. cruzi*, in parallel with a cytotoxicity assay on the human HepG2 cell line. A potent and selective 6-bromo-substituted antitrypanosomal derivative **12** was revealed, presenting EC₅₀ values of 12 and 500 nM on *T. b. brucei* trypomastigotes and *T. cruzi* amastigotes respectively, in comparison with four reference drugs (30 nM ≤ EC₅₀ ≤ 13 μM). Moreover, compound **12** was not genotoxic in the comet assay and showed high *in vitro* microsomal stability (half life >40 min) as well as favorable pharmacokinetic behavior in the mouse after oral administration. Finally, molecule **12** (E° = −0.37 V/NHE) was shown to be bioactivated by type 1 nitroreductases, in both *Leishmania* and *Trypanosoma*, and appears to be a good candidate to search for novel antitrypanosomal lead compounds.

KEYWORDS: *Trypanosoma brucei brucei*, *Trypanosoma cruzi*, 8-nitroquinolin-2(1H)-ones, redox potentials, NTR1



Human African trypanosomiasis (HAT),¹ Chagas diseases (CD),² and visceral leishmaniasis (VL)³ are infectious diseases caused by unicellular flagellated kinetoplastid parasites belonging to the *Trypanosoma* and *Leishmania* genera. From an epidemiological point of view, the World Health Organization (WHO) estimates that millions of people are at risk of contracting HAT, CD, and VL. These three diseases are also estimated to be responsible for about 30 000 annual deaths, with the caveat that these numbers may be underestimated due to the difficulty in accessing some rural areas and the unspecific symptoms during the early stage of these infections.⁴ Although these diseases are lethal if untreated, there are very few efficient and safe drugs available, each of them presenting various drawbacks for the patient (toxicity, emergence of resistances, mode of administration, treatment cost). Thus because of the lack of consideration and investments from the pharmaceutical industry, the WHO classified HAT, CD, and VL among “neglected tropical diseases” (NTDs).⁵

In this context, nitroaromatic derivatives play a key role in the fight against kinetoplastids (Figure 1). Beyond Nifurtimox and Benznidazole (antitrypanosomal drugs), nitroaromatics are fully part of the research efforts of the Drugs for Neglected Diseases initiative (DNDi). Thus among the few novel chemical entities in clinical trials against these infections,⁶ the development of fexinidazole (an orally available 5-

nitroimidazole derivative that received an agreement from the European Medicines Agency (EMA) in the treatment of HAT in 2018 and that is in phase 2 against CD),^{7–9} delamanid (a derivative that is marketed against tuberculosis and that was studied against VL),¹⁰ and DNDi-0690 (a 2-nitroimidazooxazine derivating from delamanid and that has recently entered phase-I clinical trials against VL) illustrate well the strong potential of nitroaromatic molecules in the search for novel antitrypanosomatids.¹¹

The antiparasitic mechanism of action of these molecules involves parasitic nitroreductases (NTRs). NTRs contain a flavin as a cofactor and catalyze the one- or two-electron reduction of nitrodrugs into cytotoxic electrophilic metabolites such as nitroso and hydroxylamine derivatives, which are able to form covalent adducts with DNA or proteins.¹² Two NTRs were found in *Leishmania*: a mitochondrial NTR1 catalyzing a two-electron reduction¹³ and a cytosolic NTR2 catalyzing a one-electron reduction.¹⁴ In *Trypanosoma*, only a mitochondrial type 1 NTR is expressed.^{15,16} It is important to note that

Received: December 2, 2019

Accepted: February 6, 2020

Published: February 6, 2020

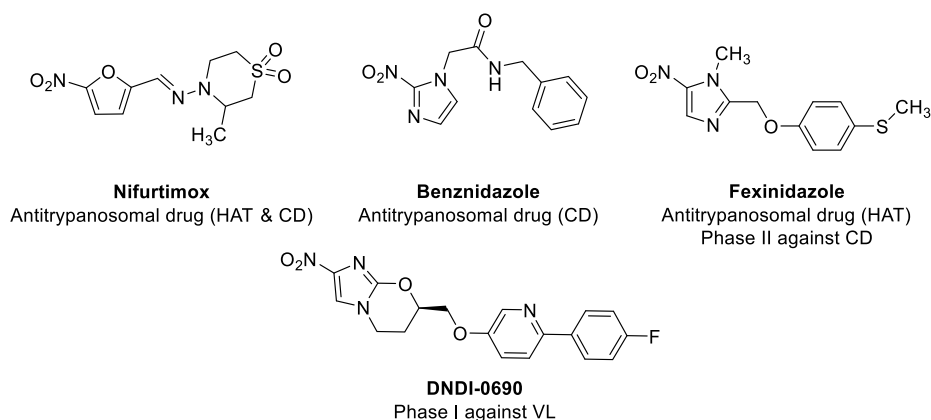


Figure 1. Structures of nitroaromatic drugs displaying antikinetoplastid activity.

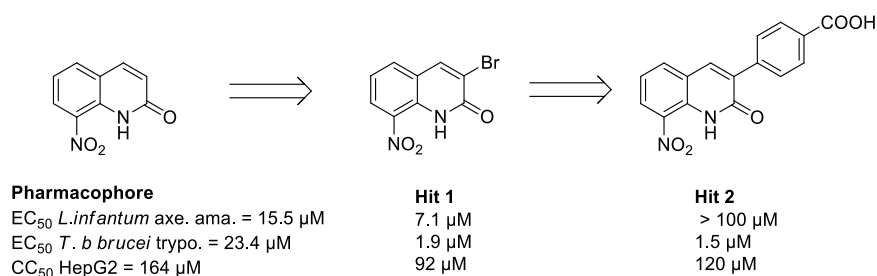
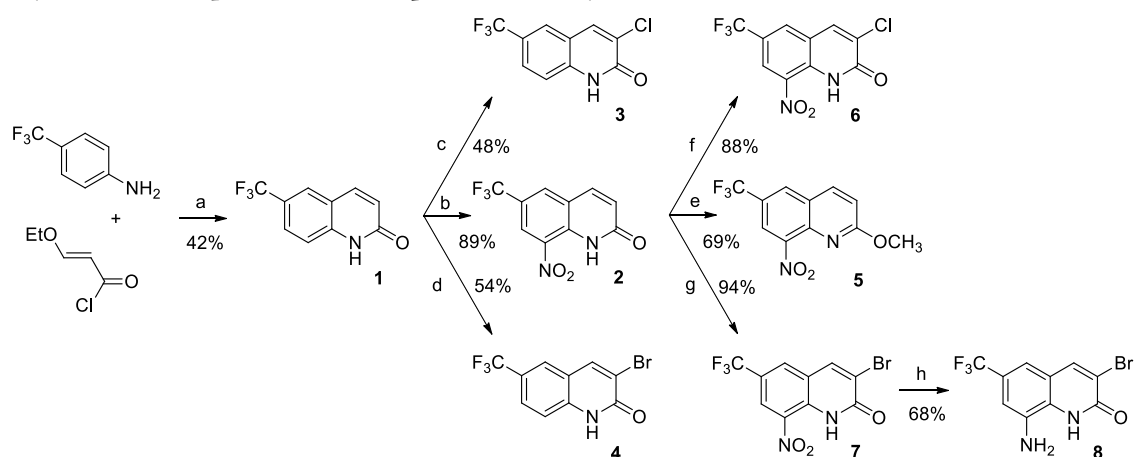


Figure 2. Antitrypanosomatid profile of previously reported 8-nitroquinolin-2(1H)-one hit compounds.

Scheme 1. Synthesis of Compounds 1–8 from *p*-Trifluoromethylaniline



these enzymes are absent from mammalian cells, an important feature for developing selective antikinetoplastid molecules. Moreover, depending on the chemical structure of nitrated derivatives, the selectivity for NTRs could be modulated. For instance, fexinidazole is selectively bioactivated by NTR1 in both *Leishmania* and *Trypanosoma*; meanwhile, delamanid is only bioactivated by NTR2 in *Leishmania*.¹⁴

In this context, by studying the antiparasitic potential of the 8-nitroquinoline scaffold,¹⁷ our research team reported a new antileishmanial pharmacophore: 8-nitroquinolin-2(1H)-one.¹⁸ After pharmacomodulation studies at position 4,^{19,20} an electrochemistry-guided work highlighted the importance of an intramolecular hydrogen bond between the nitro group and the lactam function.²¹ This work also led to the identification of a new 3-bromosubstituted antikinetoplastid hit compound derivative (**Hit 1**, Figure 2), which is bioactivated by type 1

NTRs, in both *L. donovani* and *T. brucei brucei* (*T. b. brucei*).²¹ Recently, by introducing a *p*-carboxyphenyl functionality at position 3 of the pharmacophore, we reported a new selective antitrypanosomal hit compound (**Hit 2**, Figure 2).²²

We herein present a medicinal chemistry work that greatly improved the antitrypanosomal activity of the current series via the synthesis of novel derivatives bearing electron-withdrawing groups at position 6 of the quinolinone scaffold.

To increase the oxidant character of the series and facilitate its bioactivation by nitroreductases, 15 derivatives (1–15) were prepared, bearing various electron-withdrawing groups (EWGs) at position 6. As presented in Scheme 1, eight compounds bearing a trifluoromethyl group at position 6 of the quinolinone scaffold were synthesized according to a previously reported protocol.²³ In brief, 3-ethoxyacryloyl chloride was synthesized in two steps by the saponification

Scheme 2. Synthesis of Compounds 9–15

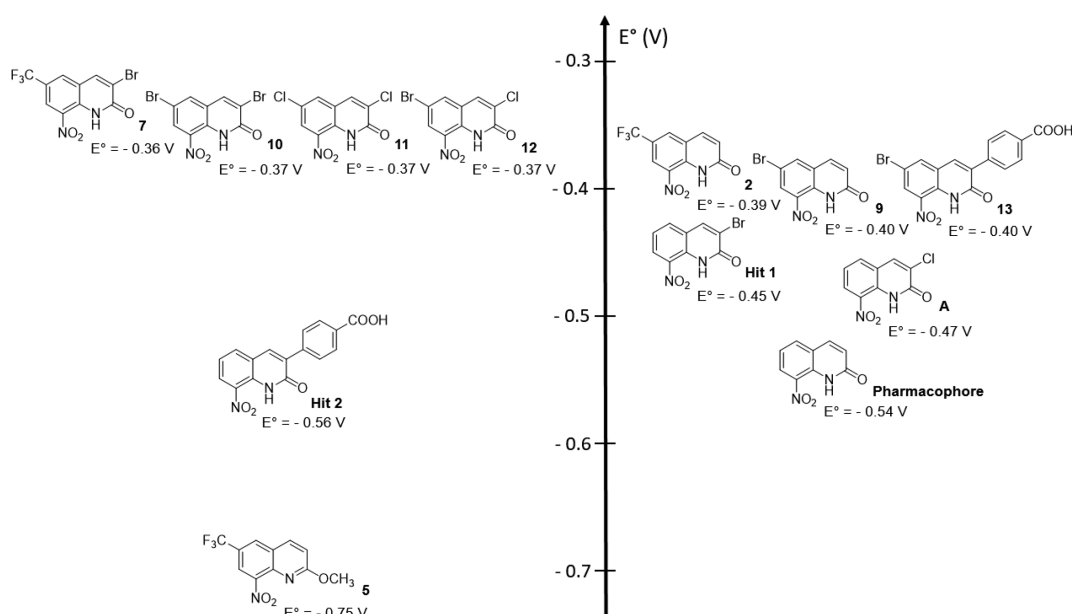
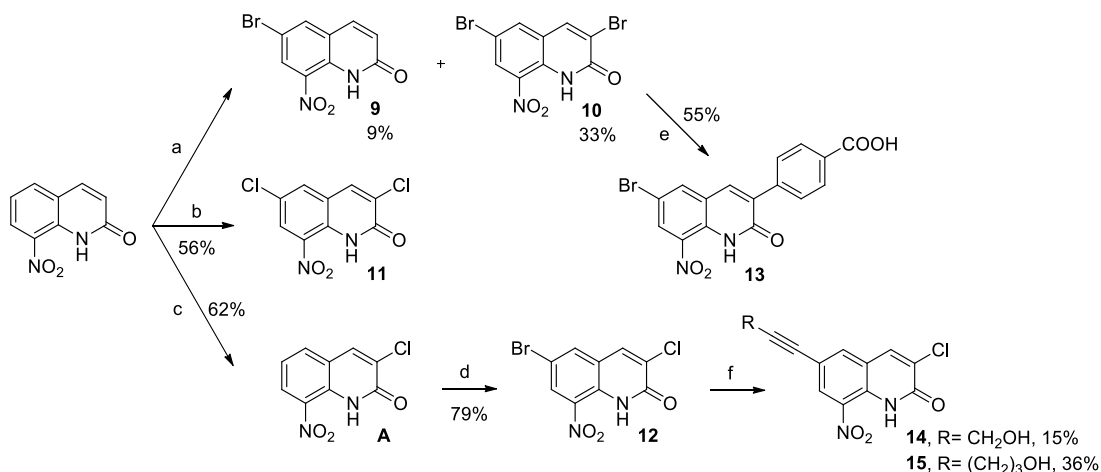


Figure 3. Redox potentials of synthesized nitroaromatic compounds determined by cyclic voltammetry.

of commercial 3,3'-diethoxyethylpropionate followed by a reaction with thionyl chloride. This acyl chloride was then reacted with *p*-trifluoromethylaniline to afford, after a cyclization step in H_2SO_4 (98%), compound **1** in 42% yield (a). Molecule **1** was then either nitrated at position 8, using classical conditions, to afford compound **2** in 89% yield (b) or selectively halogenated at position 3 to generate derivative **3** or **4** in 48 and 54% yield, respectively (c and d). The *O*-methylation of compound **2** was performed with a protocol using a mixture of methyl iodide and sodium hydride to prepare derivative **5** in 69% yield (e). Nitrated molecule **2** could also undergo chlorination at position 3, affording compound **6** in 88% yield (f), or react with NaBrO_3 in refluxing HBr , according to a previously reported protocol,²⁴ to afford halogenated derivative **7** in 94% yield (g). The nitro group of compound **7** was finally reduced to afford the amino-derivative **8**, considered as a negative control, using SnCl_2 , in 68% yield (h).

The synthesis pathway used for preparing derivatives bearing a halogen atom at position 6 of the quinolinone ring is presented in Scheme 2. It starts from 8-nitroquinolin-2(1*H*)-

one,²¹ which was reacted with bromine in refluxing acetic acid, saturated with sodium acetate, leading to a mixture of both 6-bromo and 3,6-dibromo derivatives **9** and **10** in 9 and 33% yield, respectively (a). Dichloro analogue **11** was also prepared from 8-nitroquinolin-2(1*H*)-one by reacting with 5 equiv of sodium chlorate in refluxing hydrochloric acid for 24 h (b). By using the same reaction, decreasing the amount of sodium chlorate to 3 equiv, and limiting the reaction time to 45 min, 3-chloro-8-nitroquinolin-2(1*H*)-one was formed (c).²¹ This compound could be brominated at position 6 by reacting with an excess of NaBrO_3 in refluxing HBr , leading to **12** in good yield (d). Taking into account that we previously reported the benefit of introducing a *p*-carboxyphenyl moiety at position 3 of the scaffold toward antitrypanosomal activity,²² we finally engaged dibromo-derivative **10** into a Suzuki–Miyaura reaction with *p*-(methoxycarbonyl)phenylboronic acid and then saponified the resulting ester coupling product to afford carboxylic acid **13** (e). Finally, from brominated compound **12**, derivatives **14** and **15** were obtained through a Sonogashira coupling reaction (f).

Table 1. Antikinetoplastid Activities and Cytotoxicity of Compounds 1–15

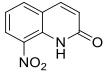
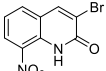
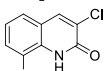
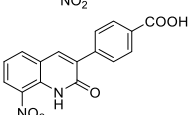
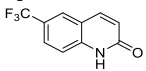
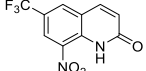
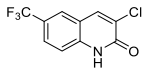
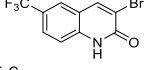
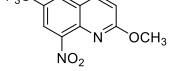
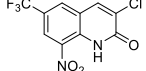
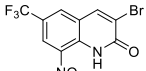
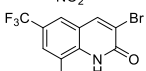
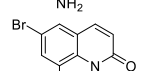
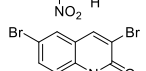
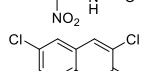
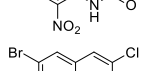
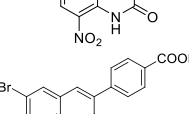
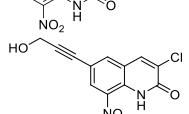
| Cpd | Structure | <i>L. infantum</i> axenic amastigote EC ₅₀ (μM) | <i>T. brucei brucei</i> trypomastigotes EC ₅₀ (μM) | Cytotoxicity HepG2 CC ₅₀ (μM) & Selectivity index regarding <i>T. b. brucei</i> |
|-------------------|-------------------------------------------------------------------------------------|------------------------------------------------------------------|---------------------------------------------------------------------|--------------------------------------------------------------------------------------------------------------|
| Phar. |  | 15.5 +/-0.5 | 23.4 +/-5.7 | 164 +/-28 7 |
| Hit 1 |  | 7.1 +/-1.5 | 1.9 +/-0.4 | 92 +/-13 48 |
| A ^[27] |  | 16 +/-0.9 | 1.2 +/-0.2 | 85 +/-4 71 |
| Hit 2 |  | > 100 ^a | 1.5 +/- 0.2 | 120 +/-7 80 |
| 1 |  | > 100 ^a | > 50 ^a | > 100 ^a ND |
| 2 |  | 18.5 +/- 3.9 | 1.7 +/- 0.9 | 41.3 +/- 3.9 24 |
| 3 |  | > 100 ^a | > 50 ^a | > 100 ^a ND |
| 4 |  | > 100 ^a | > 50 ^a | > 100 ^a ND |
| 5 |  | > 100 ^a | 20.9 +/- 14.5 | > 100 ^a >5 |
| 6 |  | 9.2 +/- 1.5 | 0.57 +/- 0.25 | 31.4 +/- 3.3 55 |
| 7 |  | 3.9 +/- 1.5 | 0.2 +/- 0.09 | 41.3 +/- 3.9 206 |
| 8 |  | > 100 ^a | 8.7 +/- 3.2 | > 100 ^a >11 |
| 9 |  | 11.6 +/- 2.5 | 0.07 +/- 0.01 | 27.9 +/- 6.0 399 |
| 10 |  | 6.5 +/- 1.8 | 0.05 +/- 0.008 | 16.6 +/- 1.2 332 |
| 11 |  | 6.2 +/- 0.6 | 0.1 +/- 0.04 | 24.3 +/- 0.9 243 |
| 12 |  | 6.7 +/- 0.8 | 0.012 +/- 0.002 | 18.1 +/- 2.5 1508 |
| 13 |  | 8.0 +/- 1.5 | 0.2 +/- 0.02 | 60.4 +/- 14.4 302 |
| 14 |  | 8.9 +/- 0.6 | 1.0 +/- 0.09 | 30.9 +/- 2.1 31 |

Table 1. continued

| Cpd | Structure | <i>L. infantum</i> axenic amastigote EC ₅₀ (μM) | <i>T. brucei brucei</i> trypomastigotes EC ₅₀ (μM) | Cytotoxicity HepG2 CC ₅₀ (μM) & Selectivity index regarding <i>T. b. brucei</i> |
|-----|-------------------------------|------------------------------------------------------------------|---------------------------------------------------------------------|--------------------------------------------------------------------------------------------------------------|
| 15 | | 10.1 +/- 1.0 | 0.85 +/- 0.1 | 32.7 +/- 0.4 38 |
| | Doxorubicin ^b | - | - | 0.2 +/- 0.02 |
| | Amphotericin B ^c | 0.06 +/- 0.001 | - | 5.5 +/- 0.25 |
| | Miltefosine ^c | 0.8 +/- 0.2 | - | 85 +/- 8.8 |
| | Fexinidazole ^{c,d,e} | 3.4 +/- 0.8 | 0.4 +/- 0.2 | > 200 ^a > 500 |
| | Suramin ^d | - | 0.03 +/- 0.009 | > 100 ^a > 3333 |
| | Eflornithine ^d | - | 13.3 +/- 2.1 | > 100 ^a > 8 |

^aEC₅₀ or CC₅₀ value was not reached at the highest tested concentration. ^bDoxorubicin was used as a cytotoxic reference drug. ^cAmphotericin B, miltefosine, and fexinidazole were used as antileishmanial reference drugs. ^dFexinidazole, suramin, and eflornithine were used as anti-*Trypanosoma brucei* reference drugs.

Electrochemistry. Because the compounds were expected to be nitroreductase substrates, we studied the influence of the introduction of EWGs at position 6 of the pharmacophore toward redox potentials. Thus redox potentials (couple R-NO₂/RNO₂^{•-}) of the synthesized compounds were measured by cyclic voltammetry in DMSO (one-electron reversible reduction). Redox potentials ranged between -0.36 and -0.75 V/NHE (Figure 3). In comparison with the original pharmacophore, the introduction of a bromine atom at position 6 (compound 9) led to a significant increase in the E° value from -0.54 to -0.40 V. The same effect was observed when a bromine atom was introduced at position 6 of hit 2 (compound 13), with an increase in the E° value of +0.16 V. It is important to note that introducing a bromine atom has a higher influence on the redox potential at position 6 (compound 9) compared with position 3 (hit 1): +0.14 versus +0.09 V. The influence of the CF₃ group toward the redox potential of the scaffold was the same as that of the bromine atom: +0.15 V (comparison between the pharmacophore and compound 2). Then, when two bromine atoms were combined at positions 3 and 6 (compound 10), a slight increase of +0.03 V was observed (no additive effect) in comparison with 6-bromo-derivative 9. Surprisingly, by comparing compounds 7 and 10–12, there was almost no effect of the variation of the EWG at position 3 or 6 toward the redox potential values, with all compounds ranging from -0.36 to -0.37 V. Finally, by comparing compound 2 with its O-methylated derivative 5, it appeared that the redox potential value was drastically lower (-0.36 V shift). This shift is not only due to the donating mesomeric effect of the methoxy group but also due to the disappearance of the intramolecular hydrogen bond between the nitro group and the lactam function.²¹

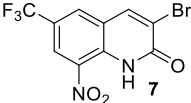
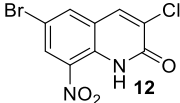
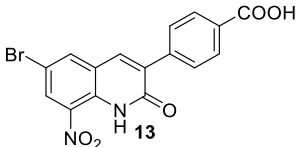
Compound Evaluation. The cytotoxicity of all compounds was first assessed on the human HepG2 cell line using doxorubicin as a positive control (Table 1). Compared with this reference drug (CC₅₀ = 0.2 μM), the series showed little (CC₅₀ = 17 μM) to no (CC₅₀ > 100 μM) cytotoxicity. Non-nitrated molecules 1, 3, and 4, O-methylated derivative 5, and 8-amino-derivative 8, considered as negative controls, displayed high CC₅₀ values, >100 μM. The results show that the

introduction of a bromine atom or a CF₃ group at position 6 of the nitrated scaffold leads to derivatives (2 and 9) that are four to five times more cytotoxic (CC₅₀ = 28–41 μM) than the 8-nitroquinolinone pharmacophore (CC₅₀ = 164 μM). When introducing an additional halogen atom at position 3 of the scaffold (6, 7, 10–12), the cytotoxicity remains close to the ones of 6-monosubstituted derivatives (CC₅₀ = 17–41 μM). Nevertheless, introducing a *p*-carboxyphenyl functionality at position 3 of the scaffold (compound 13) results in a three-fold decrease in the cytotoxicity (CC₅₀ = 60 μM) in comparison with the 3,6-dibromo derivative 10 (CC₅₀ = 17 μM).

All synthesized molecules were screened *in vitro* for their activity against *Leishmania infantum* axenic amastigotes, and their EC₅₀ values were compared with the ones of three reference drugs (amphotericin B, miltefosine, and fexinidazole) and antiketoplastid hit 1 (Table 1). Among the tested compounds, only compound 7 (E° = -0.36 V) showed a weak antileishmanial activity, displaying an EC₅₀ value of 3.9 μM in addition to a selectivity index superior to 10. Derivatives of 7 without a nitro group at position 8 of the scaffold (1, 3, 4, and 8) were inactive toward *L. infantum* as well as the O-methylated analogue 5 (E° = -0.75 V), confirming both the key role of the nitro group toward antiparasitic activity and the importance of the interaction between the nitro group and the lactam function to confer suitable redox potentials for displaying antileishmanial properties in this chemical series.²¹ Note that, contrary to hit 2, which was not active against *L. infantum* (EC₅₀ > 100 μM), the 6-bromo derivative 13 was active (EC₅₀ = 8 μM).

All molecules were also screened *in vitro* for their antitrypanosomal activity against *T. b. brucei* trypomastigotes, and their EC₅₀ values were compared with the ones of three reference drugs, suramin, eflornithine, and fexinidazole, and with antitrypanosomal hit 2. Among the 15 tested molecules, 7, 9, 10, 11, 12, and 13 displayed both submicromolar activity (12 ≤ EC₅₀ ≤ 200 nM) and good selectivity indices (SI > 200) in comparison with suramin (EC₅₀ = 30 nM), eflornithine (EC₅₀ = 13 μM), fexinidazole (EC₅₀ = 400 nM), and hit 2 (EC₅₀ = 1.5 μM). Molecule 12 was the most active and selective in the series: EC₅₀ = 12 nM and SI = 1508. Compounds without a nitro group at position 8 of the scaffold

Table 2. *In Vitro* Pharmacokinetic, Physicochemical, and Toxicological Properties of Compounds 7, 12, and 13

| |  |  |  |
|-------------------------------------------|-----------------------------------------------------------------------------------|------------------------------------------------------------------------------------|-------------------------------------------------------------------------------------|
| Microsomal stability (min) | > 40 | > 40 | > 40 |
| Albumin binding assay (%) | 99.4 | 99.0 | > 99 |
| BBB PAMPA assay (nm/s) | 450.3 ± 170.5 | 405.1 ± 69.3 | 12.7 ± 0.9 |
| cLogD ^a at pH = 7.4 | 3.24 | 2.97 | 0.44 |
| Thermodynamic solubility at pH = 7.4 (μM) | - | 21.7 +/-4.1 | - |
| Comet assay at 1 and 10 μM | - | Negative | - |

^aCalculated with MarvinSketch (ChemAxon).

appeared to be inactive (compounds 1, 3, and 4), and amino-derivative 8 was quite less active ($EC_{50} = 9 \mu M$). It is important to note that the introduction of a bromine atom at position 6 of the scaffold seems crucial to afford highly active antitrypanosomal molecules, with compound 9 being 334 times more active than the 8-nitroquinolin-2(1H)-one pharmacophore and 27 times more active than its 3-bromo-position isomer (hit 1). This key effect of the bromine atom at position 6 of the scaffold also appears when comparing the activities of 3-chloro-6-bromo hit-compound 12 with its 3-chloro-analogue A: 12 is 100 times more active than A. When comparing molecules 2 and 9, it appeared that the CF_3 group does not provide the same level of improvement in activity. Introducing an additional halogen atom at position 3 of hit molecule 9, leading to dibromo-derivative 10 and dihalo-derivative 12, afforded the most active compounds in the series ($EC_{50} = 12-50$ nM). A comparison between compound 12 and 3,6-dichlorosubstituted derivative 11 showed that the replacement of the bromine atom by a chlorine atom at position 6 was not in favor of antitrypanosomal activity. During pharmacomodulation studies at position 3 of the scaffold, hit 2 was identified as a promising antitrypanosomal hit with an EC_{50} of $1.5 \mu M$.²² When a bromine atom is introduced at position 6 of hit 2, leading to compound 13, the antitrypanosomal activity is improved, reaching an EC_{50} value of 200 nM.

Thus the molecule presenting the best antitrypanosomal profile in the series, regarding both the activity and the selectivity, was compound 12. To better evaluate its antitrypanosomal potential, an *in vitro* evaluation against intracellular *T. cruzi* amastigotes was carried out using benznidazole and fexinidazole as positive controls (Table 1). Quite interestingly, despite being about 10 times more cytotoxic than reference drugs, molecule 12 displayed a high activity ($EC_{50} = 0.5 \mu M$) against *T. cruzi*, identical to the one of benznidazole ($EC_{50} = 0.5 \mu M$) and better than the one of fexinidazole ($EC_{50} = 3 \mu M$).

To investigate more deeply the potential of compounds 7, 12, and 13 as the most active antitrypanosomal compounds of the studied series, an *in vitro* pharmacokinetic evaluation was performed, including a microsomal stability assay (female mouse microsomes), a human albumin binding assay, and a PAMPA assay using a blood-brain barrier (BBB) model (Table 2). All compounds presented good microsomal stability ($T_{1/2} > 40$ min) and strong binding to human albumin ($\geq 99\%$). However, the development of antitrypanosomal agents requires that molecules cross the BBB, as the second stage of HAT is meningoencephalitic. A PAMPA assay on a BBB model was then performed.^{25,26} Compounds 7 and 12 diffused through the lipid bilayer with Pe values significantly higher than the positive control (Pe = 450.3 and 405.1 nm/s, respectively), whereas compound 13 displayed a low Pe value (Pe = 12.7 nm/s), indicating a limited crossing of the BBB, hindering the further development of 13. This last result is not surprising because electrostatic repulsions between the negatively charged carboxylic acid group of this molecule and the negatively charged membrane constituents are probably responsible for its low permeability across the BBB in the PAMPA model. Moreover, 13 has a molecular weight approaching 400 g/mol, which could also contribute to limiting its diffusion across the BBB.²⁷ Unfortunately, the methyl ester precursor or 13 could not be evaluated *in vitro* because of a lack of aqueous solubility. The ability of hit-compound 12 to cross the BBB in the PAMPA assay is in accordance with its central nervous system multiparameter optimization (CNS MPO) score²⁸ that has a calculated value of 4.35. Finally, the aqueous solubility of hit-compound 12 was measured with a thermodynamic solubility assay at physiological pH and was determined at $21.7 \mu M$ (Table 2).

To check the antitrypanosomal mechanism of the bio-activation of compounds 7, 12 and 13, their activities were evaluated *in vitro* toward *Leishmania donovani* promastigote strains overexpressing leishmanial nitroreductases (NTR1 or NTR2). EC_{50} values were determined and compared with the ones obtained on a wild-type strain to evaluate the

bioactivation of these nitroaromatic compounds (Table 3). As reported for hit 1,²¹ compounds 7 and 12 are selectively

Table 3. Evaluation of the Bioactivation of Compounds 7, 12, and 13 by Leishmanial and Trypanosomal NTRs

| <i>Leishmania donovani</i> promastigotes EC ₅₀ (μM) | | | |
|------------------------------------------------------------------------|------------|---------------------|---------------------|
| compound | wild type | NTR1 overexpressing | NTR2 overexpressing |
| Hit 1 | 5.9 ± 0.2 | 0.47 ± 0.02 | 4.6 ± 0.12 |
| 7 | 4.1 ± 0.2 | 1.2 ± 0.05 | 4.9 ± 0.3 |
| 12 | 4.7 ± 0.09 | 0.3 ± 0.01 | 2.9 ± 0.08 |
| 13 | 2.0 ± 0.2 | 1.3 ± 0.1 | 2.1 ± 0.1 |
| <i>Trypanosoma brucei brucei</i> trypomastigotes EC ₅₀ (μM) | | | |
| compound | wild type | NTR overexpressing | |
| Hit 1 | 17.7 ± 1.0 | 3.9 ± 0.1 | |
| Hit 2 | 5.4 ± 0.12 | 4.2 ± 0.2 | |
| 7 | 6.7 ± 0.4 | 0.9 ± 0.03 | |
| 12 | 0.3 ± 0.06 | 0.02 ± 0.008 | |
| 13 | 4.0 ± 0.2 | 0.1 ± 0.009 | |
| Nifurtimox | 1.9 ± 0.05 | 0.6 ± 0.05 | |

bioactivated by leishmanial NTR1, with EC₅₀ values being 3.5 and 16 times lower on the strain overexpressing the NTR than on the wild type. Contrary to 7 and 12, compound 13 did not demonstrate significant bioactivation by NTR1 or by NTR2 in *Leishmania*. The same experiments were carried out with compounds 7, 12, and 13 on *T. b. brucei* strains overexpressing the type 1 trypanosomal NTR, comparing the EC₅₀ values with the ones determined on the wild-type strain (Table 3). All tested compounds were bioactivated by the type 1 nitroreductase of *T. b. brucei*, being, respectively, 7, 15, and 40 times more active against the strain overexpressing the NTR than against the wild type. It is interesting to note that hit 2 ($E^\circ = -0.56$ V) did not seem to be bioactivated by *T. b. brucei* NTR, whereas its 6-brominated derivative 13 ($E^\circ = -0.40$ V) was. Finally, hit-compound 12 also appeared to be six times more active than nifurtimox against *T. b. brucei*, underlining the potential of this molecule as an antitrypanosomal candidate.

Even though many safe nitroaromatic molecules are today on the market (for example, antiprotozoal 5-nitroimidazoles such as metronidazole, several antihypertensive dihydropyridines like nifedipine, some benzodiazepines like lorazepam, anti-Parkinson's catechol *O*-methyltransferase (COMT) inhibitors like entacapone, antiandrogens like flutamide, anti-inflammatory nimesulide, immunomodulating azathioprine, anticoagulant acenocoumarol, anthelmintic niclosamide, etc.) or in clinical trials (for instance, delamanid), drugs including a nitroaromatic moiety suffer from a bad reputation as possible mutagenic or genotoxic molecules, which narrows their pharmaceutical development.²⁹ The Ames test is the most commonly used assay to evaluate the mutagenic potential of compounds, using *Salmonella typhimurium* strains. However, these bacteria possess NTR, making the Ames test generally unsuitable for the evaluation of most of nitroaromatic compounds, with the genotoxicity being attributed to the reduced metabolites that are bioactivated by these bacterial enzymes (absent in human cells).³⁰ Thus it is accepted that the comet assay or the micronucleus assay are more pertinent methods to evaluate the genotoxic potential of nitroaromatic compounds. For example, fexinidazole is positive in the Ames test but negative in the micronucleus assay.³¹ A comet assay was then performed on the HepG2 cell line with hit compound

12, using methylmethanesulfonate (MMS) as a positive control (see the Supporting Information). Compound 12 was not genotoxic after 2 or 72 h of incubation or at 1 or 10 μM, concentrations chosen to be lower than its CC₅₀ on HepG2 cell line (CC₅₀ = 18 μM).

Regarding tolerance in the mouse, a once daily oral dose of compound 12, at 25 or 50 mg/kg, was administrated to eight mice (four mice in each group). These two doses were well tolerated with just a little apathy during 1 h for all mice receiving the dose of 50 mg/kg. The administration of a repeated dose of 25 mg/kg once daily for 5 days was well tolerated without any adverse effect noted. The no-observed-adverse-effect level (NOAEL)³¹ in mice was then set at 25 mg/kg/day. After euthanasia, no lesions were found on the different organs (kidney, liver, brain, heart, and lung).

Finally, the *in vivo* pharmacokinetic parameters were determined in the mouse, after oral administration at 25 mg/kg in a mixture of 5% Tween 80 and 95% of 0.5% carboxymethylcellulose in water, by using the QuEChERS method.³² Monolix Lixoft software was used to analyze the data by a noncompartmental model to fit pharmacokinetic parameters.³³ As presented in the Supporting Information (Figure S17), hit-compound 12 showed good pharmacokinetic properties: 12 is highly and rapidly absorbed after oral administration and shows good exposure. Its plasmatic half life (2.9 h) is higher than the one of the drug fexinidazole (0.8 h).³¹

Conclusions. Via an antitrypanosomal pharmacomodulation study of the 8-nitroquinolin-2(1H)-one scaffold, by introducing an EWG at positions 3 and 6 of the quinolinone ring, a novel potent antitrypanosomal hit-compound (12) was identified, displaying high activities toward *T. b. brucei* (EC₅₀ = 12 nM) and *T. cruzi* (EC₅₀ = 0.5 μM) in comparison with eflornithine (EC₅₀ = 13 μM), suramin (EC₅₀ = 30 nM), benznidazole (EC₅₀ = 0.5 μM), and fexinidazole (EC₅₀ = 0.4 and 3.0 μM). Compound 12 displays good *in vitro* pharmacokinetic parameters (good microsomal stability and BBB permeability), is rapidly absorbed after oral administration, and is well tolerated in the mouse at 25 mg/kg. Nitroaromatic hit compound 12 is selectively bioactivated by type 1 NTR in both *Leishmania* and *Trypanosoma*. An electrochemistry study showed the strong influence of the introduction of an EWG in the benzenic part of the pharmacophore toward the redox potentials and the corresponding antitrypanosomal activities. Finally, the lack of genotoxicity of compound 12 in the comet assay is an additional favorable element so as to consider further development. Compound 12 meets all criteria for an antitrypanosomal hit, as defined by Katsuno and coworkers.³⁴ *In vivo* studies on the mice model of trypanosomiasis are now planned to investigate the potential of this compound to become an antitrypanosomal lead.

■ ASSOCIATED CONTENT

Supporting Information

The Supporting Information is available free of charge at <https://pubs.acs.org/doi/10.1021/acsmchemlett.9b00566>.

Materials and methods, additional analysis of hit compounds 7, 12, and 13 as well as electrochemistry data, *in vitro* pharmacokinetics (PK) data, and *in vivo* PK data (PDF)

■ AUTHOR INFORMATION

Corresponding Author

Pierre Verhaeghe – LCC-CNRS, Université de Toulouse, CNRS, UPS, 31077 Toulouse, France; orcid.org/0000-0003-0238-2447; Phone: +33 561 333 236; Email: pierre.verhaeghe@lcc-toulouse.fr

Authors

Julien Pedron – LCC-CNRS, Université de Toulouse, CNRS, UPS, 31077 Toulouse, France

Clotilde Boudot – Université de Limoges, UMR INSERM 1094, Faculté de Pharmacie, 87025 Limoges, France

Jean-Yves Brossas – AP-HP, Groupe Hospitalier Pitié-Salpêtrière, Service de Parasitologie Mycologie, 75013 Paris, France

Emilie Pinault – Université de Limoges, BISCEM Mass Spectrometry Platform, CBRS, F-87025 Limoges, France; orcid.org/0000-0001-8811-2661

Sandra Bourgeade-Delmas – UMR 152 PharmaDev, Université de Toulouse, IRD, UPS, 31077 Toulouse, France

Alix Sournia-Saquet – LCC-CNRS, Université de Toulouse, CNRS, UPS, 31077 Toulouse, France

Elisa Boutet-Robinet – Toxalim, Université de Toulouse, INRA, ENVT, INP-Purpan, UPS, 31077 Toulouse, France; orcid.org/0000-0002-5223-4568

Alexandre Destere – Department of Pharmacology, Toxicology and Pharmacovigilance, CHU Limoges, France, INSERM, UMR 1248, University of Limoges, F-87025 Limoges, France

Antoine Tronnet – LCC-CNRS, Université de Toulouse, CNRS, UPS, 31077 Toulouse, France

Justine Bergé – LCC-CNRS, Université de Toulouse, CNRS, UPS, 31077 Toulouse, France

Colin Bonduelle – LCC-CNRS, Université de Toulouse, CNRS, UPS, 31077 Toulouse, France; orcid.org/0000-0002-7213-7861

Céline Deraeve – LCC-CNRS, Université de Toulouse, CNRS, UPS, 31077 Toulouse, France

Geneviève Pratiel – LCC-CNRS, Université de Toulouse, CNRS, UPS, 31077 Toulouse, France

Jean-Luc Stigliani – LCC-CNRS, Université de Toulouse, CNRS, UPS, 31077 Toulouse, France

Luc Paris – AP-HP, Groupe Hospitalier Pitié-Salpêtrière, Service de Parasitologie Mycologie, 75013 Paris, France

Dominique Mazier – CIMI-Paris, Sorbonne Université, 75013 Paris, France

Sophie Corvaisier – Centre d'Etudes et de Recherche sur le Médicament de Normandie (CERMN), Normandie Université, 14032 Caen, France

Marc Since – Centre d'Etudes et de Recherche sur le Médicament de Normandie (CERMN), Normandie Université, 14032 Caen, France

Aurélien Malzert-Fréon – Centre d'Etudes et de Recherche sur le Médicament de Normandie (CERMN), Normandie Université, 14032 Caen, France; orcid.org/0000-0001-6023-1861

Susan Wyllie – University of Dundee, School of Life Sciences, Division of Biological Chemistry and Drug Discovery, Dundee DD1 5EH, United Kingdom; orcid.org/0000-0001-8810-5605

Rachel Milne – University of Dundee, School of Life Sciences, Division of Biological Chemistry and Drug Discovery, Dundee DD1 5EH, United Kingdom

Alan H. Fairlamb – University of Dundee, School of Life Sciences, Division of Biological Chemistry and Drug Discovery,

Dundee DD1 5EH, United Kingdom; orcid.org/0000-0001-5134-0329

Alexis Valentin – UMR 152 PharmaDev, Université de Toulouse, IRD, UPS, 31077 Toulouse, France

Bertrand Courtioux – Université de Limoges, UMR INSERM 1094, Faculté de Pharmacie, 87025 Limoges, France

Complete contact information is available at:

<https://pubs.acs.org/10.1021/acsmchemlett.9b00566>

Author Contributions

*J.P. and C.B. contributed equally.

Notes

The authors declare no competing financial interest.

■ ACKNOWLEDGMENTS

Paul Sabatier University and the Région Occitanie are acknowledged for financial support. A.H.F., S.W., and R.M. are supported by funding from the Wellcome Trust (WT105021). C. Piveteau from Institut Pasteur de Lille, C. Bijani from Laboratoire de Chimie de Coordination de Toulouse, and C. Claparols, N. Martins-Froment, V. Bourdon, and E. Leroy from the Institut de Chimie de Toulouse are also acknowledged for their support. We also thank Dr. J.-B. Woillard for the *in vivo* pharmacokinetic analysis, Mr. F.-L. Sauvage for his help with the mass spectrometry analysis, and Dr. Ismail Belfquih for his assistance with the culture of Vero cells and *T. cruzi*.

■ REFERENCES

- (1) Büscher, P.; Cecchi, G.; Jamonneau, V.; Priotto, G. Human african trypanosomiasis. *Lancet* **2017**, *390*, 2397–2405.
- (2) Pérez-Molina, J. A.; Molina, I. Chagas disease. *Lancet* **2018**, *391*, 82–94.
- (3) Burza, S.; Croft, S. L.; Boelaert, M. Leishmaniasis. *Lancet* **2018**, *392*, 951–970.
- (4) World Health Organization. *Neglected Tropical Diseases*. https://www.who.int/neglected_diseases/diseases/en/ (accessed November 1, 2019).
- (5) Molyneux, D.; Savioli, L.; Engels, D. Neglected tropical diseases: progress towards addressing the chronic pandemic. *Lancet* **2017**, *389*, 312–325.
- (6) Drugs for Neglected Diseases Initiative (DNDi). *DNDi R&D Portfolio June 2019*. <https://www.dndi.org/diseases-projects/portfolio/> (accessed November 1, 2019).
- (7) Wyllie, S.; Patterson, S.; Stojanovski, L.; Simeons, F. R. C.; Norval, S.; Kime, R.; Read, K. D.; Fairlamb, A. H. The anti-trypanosome drug fexinidazole shows potential for treating visceral leishmaniasis. *Sci. Transl. Med.* **2012**, *4*, 119re1.
- (8) Patterson, S.; Fairlamb, A. H. Current and future prospects of nitro-compounds as drugs for trypanosomiasis and leishmaniasis. *Curr. Med. Chem.* **2019**, *26*, 4454–4475.
- (9) Mesu, V. K. B. K.; Kalonji, W. M.; Bardonneau, C.; Mordt, O. V.; Blesson, S.; Simon, F.; Delhomme, S.; Bernhard, S.; Kuziena, W.; Lubaki, J. F.; Vuvu, S. L.; Ngima, P. N.; Mbembo, H. M.; Ilunga, M.; Bonama, A. K.; Heradi, J. A.; Solomo, J. L. L.; Mandula, G.; Badibabi, L. K.; Dama, F. R.; Lukula, P. K.; Tete, D. N.; Lumbala, C.; Scherrer, B.; Strub-Wourgaft, N.; Tarral, A. Oral fexinidazole for late-stage African *Trypanosoma brucei gambiense* trypanosomiasis: a pivotal multicentre, randomised, non-inferiority trial. *Lancet* **2018**, *391*, 144–154.
- (10) Patterson, S.; Wyllie, S.; Norval, S.; Stojanovski, L.; Simeons, F. R. C.; Auer, J. L.; Osuna-Cabello, Read, K. D.; Fairlamb, A. H. The anti-tubercular drug delamanid as a potential oral treatment for visceral leishmaniasis. *eLife* **2016**, *5*, No. e09744.

- (11) Ang, C. W.; Jarrad, A. M.; Cooper, M. A.; Blaskovich, M. A. T. Nitroimidazoles: Molecular Fireworks That Combat a Broad Spectrum of Infectious Diseases. *J. Med. Chem.* **2017**, *60*, 7636–7657.
- (12) Patterson, S.; Wyllie, S. Nitro drugs for the treatment of trypanosomatid diseases: past, present, and future prospects. *Trends Parasitol.* **2014**, *30*, 289–298.
- (13) Wyllie, S.; Patterson, S.; Fairlamb, A. H. Assessing the essentiality of leishmania donovani nitroreductase and its role in nitro drug activation. *Antimicrob. Agents Chemother.* **2013**, *57*, 901–906.
- (14) Wyllie, S.; Roberts, A. J.; Norval, S.; Patterson, S.; Foth, B. J.; Berriman, M.; Read, K. D.; Fairlamb, A. H. Activation of bicyclic nitro-drugs by a novel nitroreductase (NTR2) in *Leishmania*. *PLoS Pathog.* **2016**, *12*, No. e1005971.
- (15) Hall, B. S.; Bot, C.; Wilkinson, S. R. Nifurtimox activation by trypanosomal type I nitroreductases generates cytotoxic nitrile metabolites. *J. Biol. Chem.* **2011**, *286*, 13088–13095.
- (16) Hall, B. S.; Wilkinson, S. R. Activation of Benznidazole by trypanosomal type I nitroreductases results in glyoxal formation. *Antimicrob. Agents Chemother.* **2012**, *56*, 115–123.
- (17) Verhaeghe, P.; Rathelot, P.; Rault, S.; Vanelle, P. Convenient preparation of original vinylic chlorides with antiparasitic potential in quinolone series. *Lett. Org. Chem.* **2006**, *3*, 891–897.
- (18) Paloque, L.; Verhaeghe, P.; Casanova, M.; Castera-Ducros, C.; Dumètre, A.; Mbatchi, L.; Hutter, S.; Kraiem-M'Rabet, M.; Laget, M.; Remusat, V.; Rault, S.; Rathelot, P.; Azas, N.; Vanelle, P. Discovery of a new antileishmanial hit in 8-nitroquinoline series. *Eur. J. Med. Chem.* **2012**, *54*, 75–86.
- (19) Kieffer, C.; Cohen, A.; Verhaeghe, P.; Hutter, S.; Castera-Ducros, C.; Laget, M.; Remusat, V.; M'Rabet, M. K.; Rault, S.; Rathelot, P.; Azas, N.; Vanelle, P. Looking for new antileishmanial derivatives in 8-nitroquinolin-2(1H)-one series. *Eur. J. Med. Chem.* **2015**, *92*, 282–294.
- (20) Kieffer, C.; Cohen, A.; Verhaeghe, P.; Paloque, L.; Hutter, S.; Castera-Ducros, C.; Laget, M.; Rault, S.; Valentin, A.; Rathelot, P.; Azas, N.; Vanelle, P. Antileishmanial pharmacomodulation in 8-nitroquinolin-2(1H)-one series. *Bioorg. Med. Chem.* **2015**, *23*, 2377–2386.
- (21) Pedron, J.; Boudot, C.; Hutter, S.; Bourgeade-Delmas, S.; Stigliani, J.-L.; Sournia-Saquet, A.; Moreau, A.; Boutet-Robinet, E.; Paloque, L.; Mothes, E.; Laget, M.; Vendier, L.; Pratviel, G.; Wyllie, S.; Fairlamb, A. H.; Azas, N.; Courtioux, B.; Valentin, A.; Verhaeghe, P. Novel 8-nitroquinolin-2(1H)-ones as NTR-bioactivated antikinoplastid molecules: synthesis, electrochemical and SAR study. *Eur. J. Med. Chem.* **2018**, *155*, 135–152.
- (22) Pedron, J.; Boudot, C.; Bourgeade-Delmas, S.; Sournia-Saquet, A.; Paloque, L.; Rastegari, M.; Abdoulaye, M.; El-Kashef, H.; Bonduelle, C.; Pratviel, G.; Wyllie, S.; Fairlamb, A. H.; Courtioux, B.; Verhaeghe, P.; Valentin, A. Antitrypanosomal pharmacomodulation at position 3 of the 8-nitroquinolin-2(1H)-one scaffold using pallado-catalyzed cross coupling reactions. *ChemMedChem* **2018**, *13*, 2217–2228.
- (23) Zaragoza, F.; Stephensen, H.; Peschke, B.; Rimvall, K. 2-(4-alkylpiperazin-1-yl)quinolines as a new class of imidazole-free histamine H₃ receptor antagonists. *J. Med. Chem.* **2005**, *48*, 306–311.
- (24) O'Brien, N. J.; Brzozowski, M.; Wilson, D. J. D.; Deady, L. W.; Abbott, B. M. Synthesis and biological evaluation of substituted 3-anilinoquinolin-2(1H)-ones as PDK1 inhibitors. *Bioorg. Med. Chem.* **2014**, *22*, 3781–3790.
- (25) Di, L.; Kerns, E. H.; Bezar, I. F.; Petusky, S. L.; Huang, Y. Comparison of blood-brain barrier permeability assays: in situ brain perfusion, MDR1-MDCKII and PAMPA-BBB. *J. Pharm. Sci.* **2009**, *98*, 1980–1991.
- (26) Jourdan, J. P.; Since, M.; El Kihel, L.; Lecoutey, C.; Corvaisier, S.; Legay, R.; Sopkova-de Oliveira Santos, J.; Cresteil, T.; Malzert-Fréon, A.; Rochais, C.; Dallemagne, P. Benzylphenylpyrrolizones with anti-amyloid and radical scavenging effects, potentially useful in Alzheimer's disease treatment. *ChemMedChem* **2017**, *12*, 913–916.
- (27) Van De Waterbeemd, H.; Camenisch, G.; Folkers, G.; Chretien, J. R.; Raevsky, O. A. Estimation of blood-brain barrier crossing of drugs using molecular size and shape, and H-bonding descriptors. *J. Drug Target* **1998**, *6*, 151–165.
- (28) Wager, T. T.; Hou, X.; Verhoest, P. R.; Villalobos, A. Moving beyond rules: the development of a central nervous system multiparameter optimization (CNS MPO) approach to enable alignment of druglike properties. *ACS Chem. Neurosci.* **2010**, *1*, 435–449.
- (29) Nepali, K.; Lee, H.-Y.; Liou, J.-P. Nitro-Group-Containing Drugs. *J. Med. Chem.* **2019**, *62*, 2851–2893.
- (30) Rosenkranz, E. J.; McCoy, E. C.; Mermelstein, R.; Rosenkranz, H. S. Evidence for the existence of distinct nitroreductases in *Salmonella typhimurium*: roles in mutagenesis. *Carcinogenesis* **1982**, *3*, 121–123.
- (31) Torreele, E.; Bourdin Trunz, B.; Tweats, D.; Kaiser, M.; Brun, R.; Mazué, G.; Bray, M. A.; Pécou, B. Fexinidazole - a new oral nitroimidazole drug candidate entering clinical development for the treatment of sleeping sickness. *PLoS Neglected Trop. Dis.* **2010**, *4*, No. e923.
- (32) Westland, J.; Dorman, F. QuEChERS extraction of benzodiazepines in biological matrices. *J. Pharm. Anal.* **2013**, *3*, 509–517.
- (33) Pkanalix. *Data Processing and Calculation Rules*. <http://pkanalix.lixoft.com/calculation-rules/> (accessed September 15, 2019).
- (34) Katsuno, K.; Burrows, J. N.; Duncan, K.; van Huijsduijnen, R. H.; Kaneko, T.; Kita, K.; Mowbray, C. E.; Schmatz, D.; Warner, P.; Slingsby, B. T. Hit and lead criteria in drug discovery for infectious diseases of the developing worlds. *Nat. Rev. Drug Discovery* **2015**, *14*, 751–758.

New 8-nitroquinolinone derivative displaying submicromolar *in vitro* activities against both *Trypanosoma brucei* and *cruzi*

Julien Pedron^{1#}, Clotilde Boudot^{2#}, Jean-Yves Brossas³, Emilie Pinault⁴, Sandra Bourgeade-Delmas⁵, Alix Sournia-Saquet¹, Elisa Boutet-Robinet⁶, Alexandre Destere⁷, Antoine Tronnet¹, Justine Bergé¹, Colin Bonduelle¹, Céline Deraeve¹, Geneviève Pratviel¹, Jean-Luc Stigliani¹, Luc Paris³, Dominique Mazier⁸, Sophie Corvaisier⁹, Marc Since⁹, Aurélie Malzert-Fréon⁹, Susan Wyllie¹⁰, Rachel Milne¹⁰, Alan H. Fairlamb¹⁰, Alexis Valentin⁵, Bertrand Courtioux² and Pierre Verhaeghe^{1*}

¹ LCC-CNRS, Université de Toulouse, CNRS, UPS, Toulouse, France.

² Université de Limoges, UMR INSERM 1094, Neuroépidémiologie Tropicale, Faculté de Pharmacie, 2 rue du Dr Marcland, 87025 Limoges, France

³ AP-HP, Groupe Hospitalier Pitié-Salpêtrière, Service de Parasitologie Mycologie, Paris, France.

⁴ Université de Limoges, BISCEM Mass Spectrometry Platform, CBRS, 2 rue du Pr. Descottes, F-87025 Limoges, France

⁵ UMR 152 PharmaDev, Université de Toulouse, IRD, UPS, Toulouse, France.

⁶ Toxalim (Research Centre in Food Toxicology), Université de Toulouse, INRA, ENVT, INP-Purpan, UPS, Toulouse, France

⁷ Department of Pharmacology, Toxicology and Pharmacovigilance, CHU Limoges, France, INSERM, UMR 1248, University of Limoges, France

⁸ CIMI-Paris, Sorbonne Université 91 boulevard de l'Hôpital 75013 Paris, France.

⁹ Centre d'Etudes et de Recherche sur le Médicament de Normandie (CERMN), Normandie Univ, UNICAEN F-14000 Caen, France

¹⁰ University of Dundee, School of Life Sciences, Division of Biological Chemistry and Drug Discovery, Dow Street, Dundee DD1 5EH, Scotland, United Kingdom

Table of contents

| | | |
|----|-------------------------------------------------------------|-----|
| 1. | Material and methods..... | S2 |
| 2. | Experimental spectra (NMR+HRMS) of hit-compounds 7, 12 & 13 | S23 |
| 3. | In vitro pharmacokinetic assays..... | S32 |
| 4. | Comet assay..... | S34 |
| 5. | In vivo pharmacokinetic study | S34 |
| 6. | Cyclic voltammograms..... | S36 |
| 7. | References..... | S37 |

1. Material and methods

Chemistry

All reagents and solvents were obtained from commercial sources (Fluorochem®, Sigma-Aldrich® or Alfa Aesar®) and used as received. The progress of the reactions was monitored by pre-coated thin layer chromatography (TLC) sheets ALUGRAM® SIL G/UV₂₅₄ from Macherey-Nagel and were visualized by ultraviolet light at 254 nm. The ¹H and ¹³C-NMR spectra were recorded on a Bruker UltraShield 300 MHz, a Bruker IconNMR 400 MHz, or a Bruker Avance NEO 600 MHz instrument and data are presented as follows: chemical shifts in parts per million (δ) using tetramethylsilane (TMS) as reference, coupling constant in Hertz (Hz), multiplicity by abbreviations : (s) singlet, (d) doublet, (t) triplet, (q) quartet, (dd) doublet of doublets, (m) multiplet and (br s) broad singlet. Melting points are uncorrected and were measured on a Stuart Melting Point SMP3 instrument. High-resolution mass measurements were done on a GCT Premier Spectrometer (DCI, CH₄, HRMS) or Xevo G2 QTOF (Waters, ESI+, HRMS) instrument at the Université Paul Sabatier, Toulouse. Microwave reactions were operated in a CEM Discover® microwave reactor.

Preparation of 6-trifluoromethylquinolin-2(1H)-one **1**

In a first step, 4.5 g of 3,3'-diethoxyacryloyl chloride (33.4 mmol, 1.2 equiv.), prepared from ethyl 3,3'-diethoxypropionate by a saponification followed by a reaction with SOCl₂, were added dropwise at rt onto 3.5 mL of *p*-trifluoromethylaniline (27.8 mmol, 1 equiv.) in 50 mL of dichloromethane, in the presence of 4.5 mL of pyridine (55.6 mmol, 2 equiv.). After 6 h, the reaction mixture was poured into

water, neutralized with HCl and extracted three times with dichloromethane (3×100 mL). The resulting organic layer was washed with brine, dried over anhydrous Na_2SO_4 and evaporated *in vacuo* to afford a dark oil. In a second step, the crude residue was reacted with 98% sulfuric acid (40 mL) and stirred at rt for 2 h (monitored by TLC). The reaction mixture was then poured into ice, neutralized with K_2CO_3 and extracted twice with dichloromethane (2×100 mL) and once with ethyl acetate (100 mL). The resulting organic layer was washed with water, dried over anhydrous Na_2SO_4 and evaporated *in vacuo*. The crude residue was purified by chromatography on silica gel using ethyl acetate as an eluent. Compound **1** was isolated and recrystallized in isopropanol to yield a white solid (42%, 11.68 mmol, 2.5 g).

Compound **1** ($\text{C}_{10}\text{H}_6\text{F}_3\text{NO}$): mp 201 °C, ^1H NMR (400 MHz, CDCl_3) δ : 6.83 (d, 1H, $J = 9.6$ Hz, H3), 7.54 (d, 1H, $J = 8.7$ Hz, H8), 7.76 (dd, 1H, $J = 1.8$ and 8.7 Hz, H7), 7.89 (d, 1H, $J = 1.8$ Hz, H5), 7.90 (d, 1H, $J = 9.6$ Hz, H4), 12.43 (br s, 1H, NH). ^{13}C NMR (100 MHz, CDCl_3) δ : 116.8 (CH), 119.3 (C), 122.9 (CH), 123.9 (q, $J = 271.6$ Hz, C), 125.2 (q, $J = 33.2$ Hz, C), 125.4 (q, $J = 4.1$ Hz, CH), 127.1 (q, $J = 3.4$ Hz, CH), 140.4 (C), 140.8 (CH), 164.6 (C). HRMS (DCI CH_4) calcd for $\text{C}_{10}\text{H}_7\text{F}_3\text{NO}$ $[\text{M}+\text{H}]^+$ 214.0480, found 214.0475.

Preparation of 8-nitro-6-trifluoromethylquinolin-2(1*H*)-one **2**

H_2SO_4 (98%, 10 mL) were added onto 500 mg of 6-trifluoromethylquinolin-2(1*H*)-one **1** (2.34 mmol, 1 equiv.), cooled with an ice bath. 0.96 mL of 65% HNO_3 (14.1 mmol, 5 equiv.) were then added dropwise at 0°C and the reaction mixture was stirred at rt for 2 h. The reaction mixture was successively poured into ice, neutralized with K_2CO_3 , extracted three times with dichloromethane (3×50 mL) and once with ethyl acetate (50 mL). The organic layer was washed with water, dried over anhydrous MgSO_4 and evaporated *in vacuo*. The crude residue was purified by chromatography on silica gel using ethyl acetate as an eluent. Compound **2** was isolated and recrystallized in acetonitrile to yield a pale yellow solid (89%, 2.1 mmol, 540 mg).

Compound **2** ($\text{C}_{10}\text{H}_5\text{F}_3\text{N}_2\text{O}_3$): mp 177 °C, ^1H NMR (400 MHz, CDCl_3) δ : 6.86 (dd, 1H, $J = 9.8$ and 1.9 Hz, H3), 7.85 (d, 1H, $J = 9.8$ Hz, H4), 8.12 (d, 1H, $J = 2.0$ Hz, H5), 8.73 (d, 1H, $J = 2.0$ Hz, H7), 11.33 (br s, 1H, NH). ^{13}C NMR (100 MHz, CDCl_3) δ : 122.4 (C), 122.6 (q, $J = 271.6$ Hz, C), 124.1 (q, $J = 35.2$

Hz, C), 124.8 (q, $J = 3.6$ Hz, CH), 125.2 (CH), 131.9 (q, $J = 3.4$ Hz, CH), 132.7 (C), 135.7 (C), 139.5 (CH), 161.0 (C). HRMS (ESI+) calcd for $C_{10}H_6F_3N_2O_3$ $[M+H]^+$ 259.0331 found 259.0333.

Preparation of 3-chloro-6-trifluoromethylquinolin-2(1*H*)-one **3**

A solution of 15 mL of hydrochloric acid (37%) was added onto 500 mg of 6-trifluoromethylquinolin-2(1*H*)-one **1** (2.35 mmol, 1 equiv.). The reaction mixture was then stirred at 100 °C before 300 mg of sodium chlorate (2.8 mmol, 1.2 equiv.) were added with caution (Cl_2 formation). After 7 h under reflux, the reaction mixture was left for 1 h under the hood to evacuate remaining Cl_2 vapor, and then was poured into ice, neutralized with K_2CO_3 , extracted three times with dichloromethane (3×50 mL) and once with ethyl acetate (50 mL). The organic layer was washed with water, dried over anhydrous $MgSO_4$ and evaporated *in vacuo*. The crude residue was purified by chromatography on silica gel using dichloromethane/ethyl acetate (90/10) as an eluent. Compound **3** was isolated and recrystallized in isopropanol to yield a white solid (48%, 1.1 mmol, 280 mg).

Compound **3** ($C_{10}H_5ClF_3NO$), mp 210 °C, 1H NMR (400 MHz, $CDCl_3$) δ : 7.63 (d, 1H, $J = 8.7$ Hz, H8), 7.76 (dd, 1H, $J = 8.8$ and 1.4 Hz, H7), 7.83 (d, $J = 1.4$ Hz, 1H, H5), 8.07 (s, 1H, H4), 12.6 (br s, 1H, NH). ^{13}C NMR (100 MHz, $CDCl_3$) δ : 117.0 (CH), 119.0 (C), 123.7 (C, $J = 271.8$ Hz), 124.6 (CH, $J = 4.2$ Hz), 125.9 (C, $J = 33.3$ Hz), 127.1 (CH, $J = 3.3$ Hz), 128.0 (C), 138.0 (CH), 138.9 (C), 160.3 (C). HRMS (DCI CH_4) calcd for $C_{10}H_6ClF_3NO$ $[M+H]^+$ 248.0090, found 248.0079.

Preparation of 3-bromo-6-trifluoromethylquinolin-2(1*H*)-one **4**

6-Trifluoromethylquinolin-2(1*H*)-one **1** (1.87 mmol, 400 mg) and 835 mg of *N*-bromosuccinimide (4.69 mmol, 2.5 equiv.) were added in a sealed flask of 25 mL. Then, 10 mL of acetonitrile were added and the reaction mixture was heated at 140 °C in a microwave reactor during 2 hours. The reaction mixture was poured into water and extracted three times with dichloromethane (3×50 mL). The organic layer was washed twice with a sodium carbonate solution (pH = 8) and twice with a diluted hydrochloric acid solution (pH=4), dried over anhydrous Na_2SO_4 and evaporated *in vacuo*. The crude residue was purified by chromatography on silica gel using dichloromethane/ethyl acetate (75/25) as an eluent. Compound **4** was isolated and recrystallized in acetonitrile to yield a white solid (54%, 1.0 mmol, 293 mg).

Compound **4** (C₁₀H₅BrF₃NO), mp 233 °C, ¹H NMR (400 MHz, CDCl₃) δ: 7.58 (d, 1H, *J* = 8.7 Hz, H8), 7.78 (dd, 1H, *J* = 8.7 and 1.6 Hz, H7), 7.83 (d, *J* = 1.6 Hz, 1H, H5), 8.29 (s, 1H, H4), 12.23 (br s, 1H, NH). ¹³C NMR (100 MHz, CDCl₃) δ: 116.9 (CH), 118.6 (C), 119.5 (C), 123.7 (q, *J* = 272.0 Hz, C), 124.5 (q, *J* = 4.1 Hz, CH), 125.8 (q, *J* = 33.4 Hz, C), 127.3 (q, *J* = 3.4 Hz, CH), 139.5 (C), 142.0 (CH), 160.2 (C). HRMS (ESI-) calcd for C₁₀H₄BrF₃NO [M-H]⁻ 289.9428, found 289.9433.

Preparation of 2-methoxy-8-nitro-6-trifluoromethylquinoline **5**

Under argon atmosphere, 250 mg of 8-nitro-6-trifluoromethylquinolin-2(1*H*)-one **2** (0.97 mmol, 1 equiv.) were solubilized in 5 mL of dry DMF and were added onto a DMF solution (5 mL) of 77 mg of 60% sodium hydride (1.93 mmol, 2 equiv.). After 10 min of stirring at rt, 120 μL of methyl iodide (1.93 mmol, 2 equiv.) were added dropwise. The reaction mixture was stirred at rt during 3 h, before being poured into ice and extracted four times with ethyl acetate (4 × 25 mL). The organic layer was washed twice with water, once with brine, dried over anhydrous MgSO₄ and evaporated *in vacuo*. The crude residue was purified by chromatography on silica gel using dichloromethane as eluent. Compound **5** was isolated and recrystallized in isopropanol to yield a white solid (69%, 0.66 mmol, 181 mg).

Compound **5** (C₁₁H₇N₂O₃F₃): mp 165 °C, ¹H NMR (400 MHz, CDCl₃) δ: 4.10 (s, 3H, CH₃), 7.13 (d, 1H, *J* = 8.9 Hz, H3), 8.13 (d, 1H, *J* = 8.9 Hz, H4), 8.16 (d, 1H, *J* = 2.0 Hz, H5), 8.20 (d, 1H, *J* = 2.0 Hz, H7). ¹³C NMR (100 MHz, CDCl₃) δ: 54.5 (CH₃), 116.6 (CH), 120.3 (CH, q, *J* = 3.4 Hz), 123.1 (C, q, *J* = 272.4 Hz), 125.0 (C, q, *J* = 35.0 Hz), 125.7 (C), 128.6 (CH, q, *J* = 3.98 Hz), 138.9 (CH), 139.8 (C), 146.6 (C), 165.1 (C). HRMS (DCI CH₄) calcd for C₁₁H₈N₂O₃F₃ [M+H]⁺ 273.0487, found 273.0474.

Preparation of 3-chloro-8-nitro-6-trifluoromethylquinolin-2(1*H*)-one **6**

A solution of 25 mL of hydrochloric acid (37%) was added onto 150 mg of 6-trifluoromethyl-8-nitroquinolin-2(1*H*)-one **2** (0.58 mmol, 1 equiv.). The reaction mixture was then stirred at 100 °C before 186 mg of sodium chlorate (1.74 mmol, 3 equiv.) were added with caution (Cl₂ formation). After 2 h under reflux, the reaction mixture was left for 1 h under the hood to evacuate remaining Cl₂ vapor, and then was poured into ice, neutralized with K₂CO₃, extracted three times with dichloromethane (3 × 25

mL) and once with ethyl acetate (25 mL). The organic layer was washed with water, dried over anhydrous MgSO₄ and evaporated *in vacuo*. The crude residue was isolated and recrystallized in isopropanol to yield a yellow solid (88%, 0.51 mmol, 150 mg).

Compound **6** (C₁₀H₄ClF₃N₂O₃): mp 153 °C, ¹H NMR (400 MHz, CDCl₃) δ: 8.06 (s, 1H, H4), 8.10 (d, 1H, *J* = 2.0 Hz, H5), 8.74 (d, 1H, *J* = 2.0 Hz, H7), 11.55 (br s, 1H, NH). ¹³C NMR (100 MHz, CDCl₃) δ: 122.1 (C), 122.4 (C, q, *J* = 272.6 Hz), 124.6 (C, q, *J* = 3.7 Hz), 124.9 (C, q, *J* = 35.6 Hz), 130.9 (C), 131.1 (CH, q, *J* = 3.55 Hz), 132.9 (C), 134.2 (C), 136.4 (CH), 157.0 (C). HRMS (DCI CH₄) calcd for C₁₀H₅ClF₃N₂O₃ [M+H]⁺ 292.9941, found 292.9933.

Preparation of 3-bromo-8-nitro-6-trifluoromethylquinolin-2(1*H*)-one **7**

A solution of 20 mL of hydrobromic acid (48%) was added onto 350 mg of 6-trifluoromethyl-8-nitroquinolin-2(1*H*)-one **2** (1.36 mmol, 1 equiv.). The reaction mixture was then stirred at 100 °C before 345 mg of sodium bromate (4.07 mmol, 3 equiv.) were added with caution (Br₂ formation). After 3 h under reflux, the reaction mixture was left for 1 h under the hood to evacuate remaining Br₂ vapor, and then was poured into ice, neutralized with K₂CO₃ and extracted three times with dichloromethane (3 × 50 mL). The organic layer was washed with water, dried over anhydrous Na₂SO₄ and evaporated *in vacuo*. The crude residue was purified by chromatography on silica gel using dichloromethane as an eluent. Compound **7** was isolated and recrystallized in acetonitrile to yield a pale yellow solid (94%, 1.27 mmol, 430 mg).

Compound **7** (C₁₀H₄BrF₃N₂O₃): mp 168 °C, ¹H NMR (400 MHz, CDCl₃) δ: 8.10 (d, 1H, *J* = 2.0 Hz, H5), 8.29 (s, 1H, H4), 8.76 (d, 1H, *J* = 2.0 Hz, H7), 11.51 (br s, 1H, NH). ¹³C NMR (150 MHz, CDCl₃) δ: 121.6 (C), 122.4 (C, q, *J* = 272.6 Hz), 122.5 (C), 124.7 (C, q, *J* = 3.6 Hz), 124.7 (CH, q, *J* = 35.4 Hz), 131.0 (CH, q, *J* = 3.5 Hz), 132.9 (C), 134.7 (C), 140.5 (CH), 157.1 (C). HRMS (DCI CH₄) calcd for C₁₀H₅BrF₃N₂O₃ [M+H]⁺ 336.9436, found 336.9437.

Preparation of 8-amino-3-bromo-6-trifluoromethylquinolin-2(1*H*)-one **8**

Ethanol (20 mL) was added onto 130 mg of 3-bromo-8-nitro-6-trifluoromethylquinolin-2(1*H*)-one **7** (0.38 mmol, 1 equiv.) and 365 mg of tin (II) chloride (1.92 mmol, 5 equiv.). The reaction mixture was refluxed for 5 h. The reaction mixture was then neutralized into an aqueous solution of K₂CO₃, filtered on celite, extracted twice with dichloromethane (3 × 50 mL) and once with ethyl acetate (50 mL). The combined organic layers were washed with water, dried over anhydrous MgSO₄ and evaporated *in vacuo*. The crude residue was washed with a diluted hydrochloric solution (pH = 1) three times. Compound **8** was isolated to yield an orange solid (68%, 0.26 mmol, 80 mg).

Compound **8** (C₁₀H₆BrF₃N₂O): Tdec. 238 °C, ¹H NMR (300 MHz, DMSO-d₆) δ: 6.03 (br s, 2 H, NH₂), 7.06 (d, 1 H, *J* = 2.0 Hz, H7), 7.31 (d, 1H, *J* = 2.0 Hz, H5), 8.55 (s, 1H, H4), 11.67 (br s, 1H, NH). ¹³C NMR (100 MHz, DMSO-d₆) δ: 109.6 (CH, *q*, *J* = 4.3 Hz), 112.1 (CH, *q*, *J* = 4.3 Hz), 118.3 (C), 120.0 (C), 123.9 (C, *q*, *J* = 31.9 Hz), 124.8 (C, *q*, *J* = 271.9 Hz), 127.8 (C), 136.6 (C), 142.9 (CH), 158.4 (C). HRMS (ESI +) calcd for C₁₀H₇BrF₃N₂O [M+H]⁺ 306.9694, found 306.9700.

Preparation of 6-bromo-8-nitroquinolin-2(1*H*)-one **9** and 3,6-dibromo-8-nitroquinolin-2(1*H*)-one **10**

8-Nitroquinolin-2(1*H*)-one (150 mg, 0.79 mmol, 1 equiv.) was dissolved into 25 mL of refluxing acetic acid saturated with sodium acetate. Then, 80 μL of bromine (1.58 mmol, 2 equiv.) were added dropwise and the reaction mixture was refluxed overnight. The reaction mixture was successively poured into ice, neutralized with K₂CO₃, extracted three times with dichloromethane (2 × 25 mL) and once with ethyl acetate (25 mL). The organic layer was washed with water, dried over anhydrous MgSO₄ and evaporated *in vacuo*. The crude residue was purified by chromatography on silica gel using dichloromethane/ethyl acetate (80/20) as an eluent. Compound **9** was isolated to yield a yellow solid (9%, 0.07 mmol, 20 mg) and compound **10** was isolated, after recrystallization in acetonitrile, to yield a yellow solid (33%, 0.26 mmol, 91 mg).

Compound **9** (C₉H₅BrN₂O₃): mp 230 °C, ¹H NMR (400 MHz, CDCl₃) δ: 6.79 (dd, 1H, *J* = 9.7 and 2.0 Hz, H3), 7.72 (d, 1H, *J* = 9.7 Hz, H4), 8.00 (d, 1H, *J* = 2.2 Hz, H5), 8.60 (d, 1H, *J* = 2.2 Hz, H7), 11.19 (br s, 1H, NH). ¹³C NMR (150 MHz, CDCl₃) δ: 113.4 (C), 123.5 (C), 125.0 (CH), 130.3 (CH), 132.8

(C), 133.3 (C), 137.7 (CH), 138.7 (CH), 161.0 (C). HRMS (ESI-) calcd for $C_9H_4BrN_2O_3$ [M-H]⁻ 266.9405, found 266.9402.

Compound **10** ($C_9H_4Br_2N_2O_3$): mp 202 °C, ¹H NMR (400 MHz, CDCl₃) δ: 7.96 (d, 1H, *J* = 2.2, H5), 8.16 (s, 1H, H4), 8.63 (d, 1H, *J* = 2.2, H7), 11.38 (br s, 1H, NH). ¹³C NMR (150 MHz, CDCl₃) δ: 114.1 (C), 121.3 (C), 123.5 (C), 130.4 (CH), 131.8 (C), 133.4 (C), 136.7 (CH), 139.8 (CH), 157.0 (C). HRMS (ESI-) calcd for $C_9H_3Br_2N_2O_3$ [M-H]⁻ 344.8510, found 344.8508.

Preparation of 3,6-dichloro-8-nitroquinolin-2(1*H*)-one **11**

A solution of 15 mL of hydrochloric acid (37%) was added onto 100 mg of 8-nitroquinolin-2(1*H*)-one (0.53 mmol, 1 equiv.). The reaction mixture was then stirred at 100 °C before 280 mg of sodium chlorate (2.63 mmol, 5 equiv.) were added with caution (Cl₂ formation). After 24 h under reflux, the reaction mixture was left for 1 h under the hood to evacuate remaining Cl₂ vapor, and then was poured into ice, neutralized with K₂CO₃ and extracted three times with dichloromethane (3 × 50 mL). The organic layer was washed with water, dried over anhydrous Na₂SO₄ and evaporated *in vacuo*. The crude residue was purified by chromatography on silica gel using diethyl ether as an eluent, isolated and recrystallized in acetonitrile to yield a yellow solid (56%, 0.29 mmol, 76 mg).

Compound **11** ($C_9H_4Cl_2N_2O_3$): mp 197-198 °C, ¹H NMR (400 MHz, CDCl₃) δ: 7.83 (d, 1H, *J* = 2.3 Hz, H5), 7.93 (s, 1H, H4), 8.49 (d, 1H, *J* = 2.3 Hz, H7), 11.42 (br s, 1H, NH). ¹³C NMR (100 MHz, CDCl₃) δ: 122.8 (C), 127.5 (CH), 127.7 (C), 130.6 (C), 130.9 (C), 133.3 (C), 133.9 (CH), 135.8 (CH), 157.0 (C). HRMS (DCI CH₄) calcd for $C_9H_3Cl_2N_2O_3$ [M+H]⁺ 258.9677, found 258.9672.

Preparation of 6-bromo-3-chloro-8-nitroquinolin-2(1*H*)-one **12**

A solution of 20 mL of hydrobromic acid (48%) was added onto 250 mg of 3-chloro-8-nitroquinolin-2(1*H*)-one (1.11 mmol, 1 equiv.). The reaction mixture was then stirred at 100 °C before 700 mg of sodium bromate (4.4 mmol, 4 equiv.) were added with caution (Br₂ formation). After 24 h under reflux, the reaction mixture was left for 1 h under the hood to evacuate remaining Br₂ vapor, and then was poured into ice, neutralized with K₂CO₃ and extracted three times with dichloromethane (3 × 50 mL). The organic layer

was washed with water, dried over anhydrous MgSO_4 and evaporated *in vacuo*. The crude residue was purified by chromatography on silica gel using dichloromethane as an eluent. Compound **12** was isolated and recrystallized in isopropanol to yield a yellow solid (79%, 0.88 mmol, 266 mg).

Compound **12** ($\text{C}_9\text{H}_4\text{BrClN}_2\text{O}_3$): mp 232-233 °C, ^1H NMR (400 MHz, CDCl_3) δ : 7.93 (s, 1H, H4), 7.97 (d, 1H, $J=2.2$ Hz, H5), 8.61 (d, 1H, $J=2.2$ Hz, H7), 11.41 (br s, 1H, NH). ^{13}C NMR (100 MHz, CDCl_3) δ : 114.2 (C), 123.1 (C), 130.2 (CH), 130.5 (C), 131.2 (C), 133.3 (C), 135.7 (CH), 136.8 (CH), 157.0 (C). HRMS (DCI CH_4) calcd pour $\text{C}_9\text{H}_5\text{BrClN}_2\text{O}_3$ $[\text{M}+\text{H}]^+$ 302.9172, found 302.9169.

Preparation of 6-bromo-3-(4-carboxyphenyl)-8-nitroquinolin-2(1H)-one **13**

In a sealed flask of 25 mL, 1 equiv. of 3,6-dibromo-8-nitroquinolin-2(1H)-one **10** (0.86 mmol, 300 mg), 3 equiv. of cesium carbonate (2.6 mmol, 843 mg), 0.1 equiv. of $\text{Pd}(\text{PPh}_3)_4$ (0.086 mmol, 100 mg) and 1.2 equiv. of 4-(methoxycarbonyl)phenylboronic acid (1.03 mmol, 185 mg) were added. Under argon atmosphere, 10 mL of dimethoxyethane and 2 mL of water were then added. The reaction mixture was heated at 80 °C in a microwave reactor during 2 hours. The reaction mixture was poured into water, extracted twice with dichloromethane (2×50 mL) and twice with ethyl acetate (2×50 mL). The organic layer was washed with water, dried over anhydrous MgSO_4 and evaporated *in vacuo*. The crude residue was purified by chromatography on silica gel using dichloromethane/ethyl acetate (97/3) as an eluent. 6-bromo-3-(4-carboxymethylphenyl)-8-nitroquinolin-2(1H)-one was isolated to yield a yellow solid (56%, 0.48 mmol, 195 mg). A solution of 40 mL of H_2O /Ethanol (2/8) was added onto 95 mg of this compound (0.23 mmol, 1 equiv.). Then, 47 mg of NaOH (1.18 mmol, 5 equiv.) were added and the reaction mixture was stirred at 60°C for 2 h. The reaction mixture was then poured into water, neutralized with HCl 37% and extracted three times with ethyl acetate (3×25 mL). The combined organic layers were washed with a hydrochloric solution (pH = 1), dried over anhydrous MgSO_4 and evaporated *in vacuo*. The crude residue was washed with a sodium carbonate solution (pH = 9) and compound **13** was isolated as a pale brown solid (98%, 0.22 mmol, 88 mg). Global 2-step synthesis yield from **10**= 55%.

Compound **13** ($\text{C}_{16}\text{H}_9\text{BrN}_2\text{O}_5$): Tdec. 300 °C, ^1H NMR (400 MHz, DMSO-d_6) δ : 7.90-8.06 (m, 4H, H2', H3', H5' and H6'), 8.40 (s, 1H, H4), 8.48 (d, 1H, $J=2.2$ Hz, H5), 8.54 (d, 1H, $J=2.2$ Hz, H7), 11.23 (br

s, 1H, NH), 13.08 (br s, 1H, COOH). ¹³C NMR (400 MHz, DMSO-d₆) δ: 112.8 (C), 124.00 (C), 129.3 (2xCH), 129.6 (2xCH), 129.7 (CH), 131.3 (C), 132.0 (C), 132.8 (C), 134.6 (C), 137.9 (CH), 138.1 (CH), 139.2 (C), 160.2 (C), 167.4 (C). HRMS (ESI-) calcd for C₁₆H₈BrN₂O₅ [M-H]⁻ 386.9617, found 386.9620.

Preparation of 3-chloro-6-(3-hydroxyprop-1-ynyl)-8-nitroquinolin-2(1*H*)-one **14** and 3-chloro-6-(5-hydroxypent-1-ynyl)-8-nitroquinolin-2(1*H*)-one **15**

In a sealed flask of 25 mL, 1 equiv. of 3-chloro-6-bromo-8-nitroquinolin-2(1*H*)-one **10** (0.98 mmol, 300 mg), 0.1 equiv. of CuI (0.098 mmol, 19 mg) and 0.1 equiv. of Pd(PPh₃)₄ (0.098 mmol, 113 mg) were added. Under argon atmosphere, anhydrous dimethoxyethane (10 mL), Et₃N (401 μL, 2.94 mmol, 3 equiv) and the appropriate alkyne (1.47 mmol, 1.5 equiv) were successively added. The reaction mixture was heated at 100 °C during 1 hour. The reaction mixture was poured into water, extracted twice with dichloromethane (2 × 50 mL) and twice with ethyl acetate (2 x 50 mL). The organic layer was washed with water, dried over anhydrous Na₂SO₄ and evaporated in vacuo. The crude residue was purified by chromatography on silica gel using dichloromethane/ethyl acetate (80/20) as an eluent and recrystallized to give compounds **14** and **15**.

Compound **14** (C₁₂H₇ClN₂O₄) was recrystallized from isopropanol, as a beige solid in 15% yield (41 mg). Tdec. = 148 °C, ¹H NMR (400 MHz, DMSO-d₆) δ: 4.35 (m, 3H), 8.18 (d, 1H, *J* = 1.9 Hz, H5), 8.31 (d, 1H, *J* = 1.9 Hz, H7), 8.48 (s, 1H, H4), 11.48 (br s, 1H, NH). ¹³C NMR (100 MHz, DMSO-d₆) δ: 49.8 (CH₂), 81.1 (C), 92.0 (C), 116.5 (C), 122.0 (CH), 128.0 (C), 129.8 (CH), 131.4 (C), 134.6 (C), 137.3 (CH), 137.8 (CH), 157.1 (C). HRMS (ESI+) calcd for C₁₂H₈ClN₂O₄ [M+H]⁺ 279.0173, found 279.0185.

Compound **15** (C₁₄H₁₁ClN₂O₄) was recrystallized from isopropanol, as a yellow solid in 36% yield (108 mg). Tdec. = 176 °C, ¹H NMR (400 MHz, DMSO-d₆) δ: 1.67-1.71 (m, 2H, CH₂), 2.50-2.54 (m, 2H, CH₂), 3.50-3.56 (q, 2H, *J* = 17.6 Hz, CH₂), 4.54-4.56 (t, 1H, *J* = 10.3 Hz, OH), 8.17 (d, 1H, *J* = 1.9 Hz, H5), 8.30 (d, 1H, *J* = 1.9 Hz, H7), 8.47 (s, 1H, H4), 11.47 (br s, 1H, NH). ¹³C NMR (100 MHz, DMSO-d₆) δ: 15.8 (CH₂), 31.7 (CH₂), 59.8 (CH₂), 77.8 (C), 93.1 (C), 117.4 (C), 122.0 (C), 127.9 (C), 129.85

(CH), 131.1 (C), 134.5 (C), 137.3 (CH), 137.75 (CH), 157.1 (C). HRMS (ESI+) calcd for C₁₄H₁₂ClN₂O₄ [M+H]⁺ 307.0486, found 307.0480.

Electrochemistry

Voltammetric measurements were carried out with a potentiostat Autolab PGSTAT100 (ECO Chemie, The Netherlands) controlled by GPES 4.09 software. Experiments were performed at room temperature in a homemade airtight three-electrode cell connected to a vacuum/argon line. The reference electrode consisted of a saturated calomel electrode (SCE) separated from the solution by a bridge compartment. The counter electrode was a platinum wire of approximately 1 cm² apparent surface. The working electrode was GC microdisk (1.0 mm of diameter – Biologic SAS). The supporting electrolyte tetrabutylammonium hexafluorophosphate (*n*Bu₄N[PF₆], Fluka, 99% puriss electrochemical grade) and the solvent DMSO (Sigma-Aldrich puriss p. a. dried <0.02% water) were used as received and simply degassed under argon. The solutions used during the electrochemical studies were typically 10⁻³ M in compound and 0.1 M in supporting electrolyte. Before each measurement, the solutions were degassed by bubbling Ar and the working electrode was polished with a polishing machine (Presi P230). Under these experimental conditions employed in this work, the half-wave potential ($E_{1/2}$) of the ferrocene Fc⁺/Fc couple in DMSO was $E_{1/2} = 0.45$ V vs SCE. The redox potentials measured (V/SCE) correspond to the reversible one-electron reduction/oxidation of the redox couple nitro group/anion radical and were corrected versus the normal hydrogen electrode (+ 0.241 V).

Biology

Antileishmanial activity on L. infantum axenic amastigotes.^[1]

L. infantum promastigotes (MHOM/MA/67/ITMAP-263, CNR Leishmania, Montpellier, France, expressing luciferase activity) were cultivated in RPMI 1640 medium supplemented with 10% foetal calf serum (FCS), 2 mM L-glutamine and antibiotics (100 U/mL penicillin and 100 µg/mL streptomycin) and harvested in logarithmic phase of growth by centrifugation at 900 g for 10 min. The supernatant was removed carefully and was replaced by the same volume of RPMI 1640 complete medium at pH 5.4 and incubated for 24 h at 24 °C. The acidified promastigotes were then incubated for 24 h at 37 °C

in a ventilated flask to transform promastigotes into axenic amastigotes. The amastigote stage was checked both by electron microscopy (short flagellum with small bulbous tip extending beyond a spherical cell body) and RT-PCR for confirming the overexpression of ATG8 and amastin genes in amastigotes, compared to promastigotes. The effects of the tested compounds on the growth of *L. infantum* axenic amastigotes were assessed as follows. *L. infantum* amastigotes were incubated at a density of 2×10^6 parasites/mL in sterile 96-well plates with various concentrations of compounds dissolved in DMSO (final concentration less than 0.5% v/v), in duplicate. Appropriate controls DMSO, amphotericin B, miltefosine and fexinidazole (reference drugs purchased from Sigma Aldrich) were added to each set of experiments. After a 48 h incubation period at 37 °C, each plate-well was then microscopically-examined to detect any precipitate formation. To estimate the luciferase activity of axenic amastigotes, 80 µL of each well were transferred to white 96-well plates, Steady Glow® reagent (Promega) was added according to manufacturer's instructions, and plates were incubated for 2 min. The luminescence was measured in Microbeta Luminescence Counter (PerkinElmer). Efficient concentration 50% (EC₅₀) was defined as the concentration of drug required to inhibit by 50% the metabolic activity of *L. infantum* amastigotes compared to control. EC₅₀ values were calculated by non-linear regression analysis processed on dose response curves, using TableCurve 2D V5 software. EC₅₀ values represent the mean of three independent experiments.

Antileishmanial activity on L. donovani promastigotes NTR1 and NTR2 over-expressing strain.

Cell lines and culture conditions: The clonal *Leishmania donovani* cell line LdBOB (derived from MHOM/SD/62/1S-CL2D) was grown as promastigotes at 26 °C in modified M199 media, as previously described.^[2] LdBOB promastigotes overexpressing NTR1 (LinJ.05.0660)^[3] and NTR2 (LinJ.12.0730)^[4] were grown in the presence of nourseothricin (100 µg/mL). To examine the effects of test compounds on growth, triplicate promastigote cultures were seeded with 5×10^4 parasites/mL. Parasites were grown in 10 ml cultures in the presence of drug for 72 h, after which 200 µL aliquots of each culture were added to 96-well plates, 50 µM resazurin was added to each well and fluorescence (excitation of 528 nm and emission of 590 nm) measured after a further 4 h incubation^[5]. Data were processed using GRAFIT (version 5.0.4; Erithacus software) and fitted to a 2-parameter equation, where the data are

corrected for background fluorescence, to obtain the concentration inhibiting growth by 50% (EC₅₀): In this equation [I] represents inhibitor concentration and m is the slope factor. Experiments were repeated at least two times and the data are presented as the weighted mean plus standard deviation.

$$y = \frac{100}{1 + \left(\frac{[I]}{IC_{50}} \right)^m}$$

Antitrypanosomal activity on T. brucei brucei trypomastigotes.

Assays were performed on *Trypanosoma brucei brucei* AnTat 1.9 strain (IMTA, Antwerpen, Belgium). It was cultured in MEM with Earle's salts, supplemented according to the protocol of Baltz et al.^[6] with the following modifications, 0.5 mM mercaptoethanol (Sigma Aldrich[®], France), 1.5 mM L-cysteine (Sigma Aldrich[®]), 0.05 mM bathocuproïne sulfate (Sigma Aldrich[®]) and 20% heat-inactivated horse serum (Gibco[®], France), at 37°C in an atmosphere of 5% CO₂. The parasites were incubated at an average density of 2000 parasites/well in sterile 96-wells plates (Mc2[®], France) with various concentrations of compounds dissolved in DMSO (Sigma Aldrich[®]), in duplicate. Reference drugs suramin, eflornithine, and fexinidazole (purchased from Sigma Aldrich, France and Fluorochem, UK) dissolved in NaCl 0.9% or DMSO, were added to each set of experiments. The effects of the tested compounds were assessed by the viability marker Alamar Blue[®] (Fisher, France) assay described by Rüz et al.^[7] After a 69 h incubation period at 37 °C, 10 µL of Alamar Blue[®] was then added to each well, and the plates were incubated for 5h.^[8] The plates were read in a PerkinElmer ENSPIRE (Germany) microplate reader using an excitation wavelength of 530 nm and an emission wavelength of 590 nm. EC₅₀ were calculated by nonlinear regression analysis processed on dose-response curves, using GraphPad Prism software (USA). EC₅₀ was defined as the concentration of drug necessary to inhibit by 50% the viability of *T. brucei brucei* compared to the control. EC₅₀ values were calculated from three independent experiments in duplicate.

Antitrypanosomal evaluation on the development of T. cruzi amastigotes

Vero cells (normal kidney epithelial cells of *Cercopithecus aethiops*) were obtained from the Virology Laboratory of the Pitié Salpêtrière Hospital (Paris, France). At late exponential growth phase, trypsin-treated Vero cells were subcultured every seven days in RPMI-1640 medium (Life technologies) supplemented with streptomycin/penicillin (Life technologies) and 5% heat-inactivated foetal bovine serum (FBS) (Life technologies). Subcultures were maintained at 37°C in a humidified atmosphere of 5% CO₂. CL Brener strain (collection number: MNHN-CEU- 2016-0159) was a gift from Pr. P. Grellier of the Muséum National d'Histoire Naturelle (Paris, France). *T. cruzi* stocks were maintained by weekly passage in Vero cells. Infectious trypomastigotes were collected from culture supernatants.

Then, sterile, 96-well plates were seeded with exponentially growing Vero cells (40,000 cells per cm² in 2, 2 mL RPMI with serum per well) harvested from the preceding subcultures, were added to each well. After incubation at 37°C for 2 days in 5% CO₂ in air, the cells were infected with *T. cruzi* trypomastigotes in ratio 3:1 (parasites : host cells). After 24 hours, the non-infecting trypomastigotes removed by washing twice with HBSS buffer (without Ca²⁺ and Mg²⁺) and the chemical compounds in completed RPMI media were added immediately, to be tested to their inhibitory effects on parasite growth and development. Culture plates were incubated for an additional 120 h at 37°C with 5% CO₂. Three replicate wells for each condition were done. On days 5 and 6 post-infection, trypomastigotes were released from the cells. On day 6, the culture medium was removed and transferred to a centrifuge tube. Attached infected cells were washed with 5 mL of HBSS buffer. The culture medium and wash containing trypomastigotes were mixed and centrifuged at 1000 g for 15 min at room temperature. Subsequently, trypomastigotes re-suspended in 2 mL and counted in a haemocytometer (Kova cells) using a light microscope. For 50% effective concentration (EC₅₀) determinations, compounds were serially diluted 2 to 4-fold in RPMI media, with final assay concentrations ranging from 0,1 to 25 µM. The 50% inhibiting concentrations (EC₅₀), defined as the drug concentration that resulted in a 50% reduction of trypomastigotes compared to the non-treated controls was estimated by non-linear regression analysis. EC₅₀ values represent the mean value calculated from two independent experiments that were performed in triplicate.

Antitrypanosomal activity on T. brucei trypomastigotes overexpressing the nitroreductase (NTR1).

Trypanosoma brucei bloodstream-form 'single marker' S427 (T7RPOL TETR NEO) and drug-resistant cell lines were cultured at 37°C in HMI9-T medium^[9] supplemented with 2.5 µg/mL G418 to maintain expression of T7 RNA polymerase and the tetracycline repressor protein. Bloodstream trypanosomes overexpressing the *T. brucei* nitroreductase (NTR1)^[10] were grown in medium supplemented with 2.5 µg/mL phleomycin and expression of NTR was induced by the addition of 1 µg/mL tetracycline. Cultures were initiated with 1×10^5 cells ml⁻¹ and sub-cultured when cell densities approached 1–2 ($\times 10^6$)/mL. In order to examine the effects of inhibitors on the growth of these parasites, triplicate cultures containing the inhibitor were seeded at 1×10^5 trypanosomes/mL. Cells overexpressing NTR were induced with tetracycline 48 h prior to EC₅₀ analysis. Cell densities were determined after culture for 72 h, as previously described^[11]. EC₅₀ values were determined using GraFit as described above.

Cytotoxic evaluation on HepG2 cell line.

The evaluation of the molecules cytotoxicity on the HepG2 (hepatocarcinoma cell line from ECACC purchased from Sigma-Aldrich, ref 85011430-1VL certificated without mycoplasma) was done according to the method of Mosman with slight modifications.^[12] Briefly, cells (1×10^5 cells/mL) in 100 µL of complete medium, [Alpha MEM Eagle from PAN BIOTECH supplemented with 10% foetal bovine serum, 2 mM L-glutamine and antibiotics (100 U/mL penicillin and 100 µg/mL streptomycin)] were seeded into each well of 96-well plates and incubated at 37 °C and 5% CO₂. After a 24 h incubation, 100 µL of medium with various product concentrations and appropriate controls were added and the plates were incubated for 72 h at 37 °C and 5% CO₂. Each plate-well was then microscope-examined for detecting possible precipitate formation before the medium was aspirated from the wells. A MTT solution (100 µL, 0.5 mg/mL in Alpha MEM Eagle) was then added to each well. Cells were incubated for 2 h at 37 °C and 5% CO₂. After this time, the MTT solution was removed and DMSO (100 µL) was added to dissolve the resulting formazan crystals. Plates were shaken vigorously (300 rpm) for 5 min. The absorbance was measured at 570 nm with a microplate spectrophotometer (Eon BioTek). DMSO was used as blank and doxorubicin (purchased from Sigma Aldrich) as positive control. CC₅₀ were

calculated by non-linear regression analysis processed on dose response curves, using TableCurve 2D V5 software. CC₅₀ values represent the mean value calculated from three independent experiments.

Comet assay

The alkaline comet assay was used to detect DNA strand breaks and alkali-labile sites. Trypsinized HepG2 cells were embedded in 0.7% low-melting point agarose (Sigma “Low Gelling Temperature”) and laid on pre-cut sheets of polyester film (Gelbond® film) to perform minigel deposits as previously described [13]. Films were then placed in lysis solution (2.5 M NaCl, 0.1 M Na₂EDTA, 10 mM Tris, 1 % Triton X-100, 10 % DMSO pH 10) for 18 h at 4 °C. Electrophoresis (with a solution which contained 0.3 M NaOH, 1 mM Na₂EDTA, pH > 13) was processed for 24 min in a tank with a power supply giving 28 V (resulting in 0.8 V/cm). After electrophoresis, films were immersed 2 × 5 min in PBS for neutralization, followed by fixation in 100% ethanol for 1.5 h and drying. After staining with SYBR® Gold (Life Technologies) at 10 000 × dilution for 20 min, films were observed at 20x magnification with an epifluorescence microscope equipped with an automated platform (Nikon NiE) and coupled to a camera (DS-Q1Mc) and the software Nikon NiS Element Advanced Research to automatically capture images. In these images, for each cell, the level of DNA damage was evaluated using a semi-automated scoring system, by measurement of the intensity of all tail pixels divided by the total intensity of all pixels in head and tail of comet, by means of the software “Lucia comet assay” (Laboratory Imaging, Prague Czech Republic). Fifty cells per deposit and two deposits *per* sample were analyzed. The median from these 100 values was calculated and named “% tail DNA”.

Parallel Artificial Membrane Permeability Assay (PAMPA)^[14,15]

The PAMPA-BBB experiments were conducted using the Pampa Explorer Kit (Pion Inc) according to manufacturer's protocol. Briefly, each stock compound solution (20 mM in DMSO) were diluted in Prisma HT buffer pH 7.4 (Pion Inc) to 100 µM. 200 µL of this solution (n = 6) were added to donor plate (P/N 110243). BBB-1 Lipid (5 µL, P/N 110672) was used to coat the membrane filter of the acceptor plate (P/N 110243). Brain Sink Buffer (200 µL, P/N 110674) was added to each well of the acceptor plate. The sandwich was incubated at room temperature for 4h, without stirring. After the

incubation the UV-visible spectra were measured with the microplate reader (Tecan infinite M200), and the permeability value (Pe) was calculated by the PAMPA Explorer software v.3.7 (pION) for each compound. The corticosterone and the theophylline were used as references.

Solubility determination at pH 7.4.

Thermodynamic solubility at pH 7.4 of molecule **12** was determined according to the classical shake-flask method (Organisation for Economic Cooperation and Development guideline n° 105) and a miniaturized procedure. [16] Phosphate Buffer solutions (pH 7.4, 10 μ M, ionic strength 50 mM) were prepared from Na₂HPO₄, KH₂PO₄ and KCl (Sigma Aldrich, Saint Quentin Fallavier, France); 10 μ L of 50 mM stock solution was added to 1.5 mL microtubes containing 990 μ L buffer (n = 4). Tubes were briefly sonicated and shaken by inversion during 24 h at room temperature. Then, microtubes were centrifuged at 12,225 \times g for 5 min; 100 μ L supernatant was mixed with 100 μ L acetonitrile in a Greiner UV microplate. Standard solutions were prepared extemporaneously diluting 25 mM DMSO stock solutions at 0, 5 and 12.5 mM; 5 μ L each working solution was diluted with 995 μ L buffer and 100 μ L was then mixed in microplate with 100 μ L acetonitrile to keep unchanged the final proportions of each solvent in standard solutions and samples. Determination of solubility at pH 7.4 was made with a Synergy 2 (Biotek, Colmar, France) microplate reader in spectrophotometric mode (230 to 450 nm) from the specific λ_{max} of each compound. The calibration curve obtained from the three standard solutions of tested compounds at 0, 25, and 50 μ M in a 50:50 (vol/vol) mixture of buffer with acetonitrile/DMSO (99:1; vol/vol). Calibration curves were linear with $R^2 > 0.99$.

Microsomal stability protocol.

The compounds and propranolol, used as reference, are incubated in duplicate (reaction volume of 0.5 mL) with female mouse microsomes (CD-1, 20 mg / ml, BD Gentest™) at 37 °C in a 50 mM phosphate buffer, pH 7.4, in the presence of MgCl₂ (5 mM), NADP (1 mM), glucose-6-phosphate dehydrogenase (0.4 U/mL) and glucose-6-phosphate (5 mM). For the estimation of the intrinsic clearance: 50 μ L aliquot at 0, 5, 10, 20, 30 and 40 min are collected and the reaction is stopped with 4 volumes of acetonitrile (ACN) containing the internal standard. After centrifugation at 10000 g, 10 min, 4 °C, the supernatants

are kept at 4 °C for immediate analysis or placed at -80 °C in case of postponement of the analysis. Controls (t_0 and t_{final}) in triplicate are prepared by incubation of the internal standard with microsomes denatured by acetonitrile. The LC-MS used for this study is a Waters® Acquity I-Class / Xevo TQD, equipped with a Waters® Acquity BEH C18 column, 50 x 2.1 mm, 1.7 μm. The mobile phases are (A) ammonium acetate 10 mM and (B) acetonitrile with 0.1% formic acid. The injection volume is 1 μL and the flow rate is 600 μL/min. The chromatographic analysis, total duration of 4 min, is made with the following gradient: 0 < t < 0.2 min, 2% (B); 0.2 < t < 2 min, linear increase to 98% (B); 2 < t < 2.5 min, 98% (B); 2.5 < t < 2.6 min, linear decrease to 2% (B); 2.6 < t < 4 min, 2% (B). Compound 8-bromo-6-chloro-3-nitro-2-(phenylsulfonylmethyl)imidazo[1,2-*a*]pyridine is used as internal standard. The quantification of each compound is obtained by converting the average of the ratios of the analyte/internal standard surfaces to the percentage of consumed product. The ratio of the control at t_0 corresponds to 0% of product consumed. The calculation of the half-life ($t_{1/2}$) of each compound in the presence of microsomes is done according to the equation: $t_{1/2} = \frac{\ln(2)}{k}$. Where k is the first-order degradation constant (the slope of the logarithm of compound concentration versus incubation time). The intrinsic clearance *in vitro* (Cl_{int} expressed in μL/min/mg) is calculated according to the equation:

$$Cl_{\text{int}} = \frac{\text{dose}}{\text{AUC}_{\infty}} / [\text{microsomes}]$$

Where dose is the initial concentration of product in the sample, AUC_{∞} is the area under the concentration-time curve extrapolated to infinity and [microsomes] is the microsome concentration expressed in mg/μL.

Plasma protein binding procedure.

The plasma doped with the tested compound is incubated at 37 °C in triplicate in one of the compartments of the insert, the other compartment containing a phosphate buffer solution at pH 7.2. After stirring for 4 h at 300 rpm, a 25 μL aliquot of each compartment is taken and diluted; the dilution solution is adapted to obtain an identical matrix for all the compartments after dilution. In parallel, the reprocessing of a plasma doped but not incubated will allow to evaluate the recovery of the study. The LC-MS used for this study is a Waters® Acquity I-Class / Xevo TQD, equipped with a Waters® Acquity

BEH C18 column, 50 × 2.1 mm, 1.7 μm. The mobile phases are (A) ammonium acetate 10 mM and (B) acetonitrile with 0.1% formic acid. The injection volume is 1 μL and the flow rate is 600 μL/min. The chromatographic analysis, total duration of 4 min, is made with the following gradient: 0 < t < 0.2 min, 2% (B); 0.2 < t < 2 min, linear increase to 98% (B); 2 < t < 2.5 min, 98% (B); 2.5 < t < 2.6 min, linear decrease to 2% (B); 2.6 < t < 4 min, 2% (B). Carbamazepine, oxazepam, warfarine and diclofenac are used as reference drugs and Propranolol is used as internal standard. The unbound fraction (fu) is

calculated according to the following formula: $f_u = \frac{A_{\text{Plasma, 4h}} - A_{\text{PBS, 4h}}}{A_{\text{Plasma, 4h}}} \times 100$. The percentage of recovery

is calculated according to the following formula: $\% \text{ Recovery} = \frac{(V_{\text{PBS}} \times A_{\text{PBS, 4h}}) + (V_{\text{Plasma}} \times A_{\text{Plasma, 4h}})}{(V_{\text{Plasma}} \times A_{\text{Plasma, 0h}})}$.

Where A is the ratio of the area under peak of the studied molecule and the area under peak of the internal standard (propranolol 200 nM). V is the volume of solution present in the compartments (VPBS = 350 μL and Vplasma = 200 μL).

In vivo analysis

Female Swiss mice of 8 weeks (weight 30-32 g) are used. All animals were kept under the same conditions according to laboratory animal care guidelines (European convention SPE123), and all protocol are approved by the ethical committee and the Ministry of Higher Education, Research and Innovation with the agreement number APAFIS#19730-2019031215178087 v1.

Four mice received 50 μL of the **12** suspension by oral route at 25 mg/kg (the tolerated dose). One hundred microliters of blood were taken from tail and collected into micro tubes with heparin at 0.5, 1, 3, 6, 9, 12, and 24h after administration. Blood samples were stored frozen until required for assay.

Sample preparation for spectrometry analysis

Megazol was used like the internal standard (IS). LC-MS Optima grade Acetonitrile (ACN) and Methanol (MeOH), acetic acid and formic acid (FA) were purchased from Fisher Scientific. Ready-to-use QuEChERS salts (6 g MgSO₄/1.5 g NaCl/1.5 g sodium citrate dihydrate/750mg sodium citrate sesquihydrate) were supplied by VWR.

200 µl of ACN containing megalol (IS) at a concentration of 625 ng/ml were added to 100 µl blood samples. The mixture was vortexed during 30 sec. After 10 min, 40 mg of QuEChERS salts were added. Samples were briefly vortexed and centrifuged at 16,000g for 10 min. Ten microliters of the upper layer was directly transferred in an injection vial before being diluted (1/10; v/v) in a 0.1 % formic acid in water. Finally, 5µL was injected in the LC-MS-MS system.

Calibrations standards (8 levels, from 10 to 1,000ng/ml) and quality controls (QC) (75 and 625 ng/ml) were obtained by adding appropriate 20X working standard solutions in blank whole blood. [17, 18]

LC-MS/MS conditions

The chromatographic system consisted in two Shimadzu LC-30 AD pumps (NexeraX2), a CTO 20AC oven, and a SIL-30AC autosampler (Shimadzu, Marne-la-Vallée, France). Chromatographic separation was performed using a EC-C8 column (Poroshell 120, 2.1 mm x 75 mm, 2.7 µM; Agilent) at a flow rate of 0.25ml/min using a gradient of 0.1% acetic acid in water (A) and 0.1% acetic acid in MeOH/ACN 50:50 (B) programmed as follows: 0.0–0.1, 20% (B); 0.1–1.0, 20 to 70% (B); 1.0–4.0, 70% to 100% (B); 4.0–5.5, 100% (B); 5.5–6.0, 100 to 20% (B); and 6.0–8.0 column equilibration with 20% (B). Oven temperature was set at 60 °C.

A Shimadzu 8060 triple quadrupole mass spectrometer was used in the negative electrospray ionization mode. The main common parameter settings were as follows: interface voltage, 1.5kV; nebulizing gas flow, 3 L/min; heating gas flow, 10 L/min; interface temperature, 300°C; desolvation line (DL) temperature, 250°C; heat block temperature, 400°C; and drying gas flow, 10 L/min. Multiple-reaction monitoring (MRM) transitions and specific parameters are presented in Table 1. All parameters (collision energy, Q1/Q3 pre-bias) were optimized from standard flow injection analysis. Dwell time was set at 100ms per transition.

Table 1: LC retention time (RT) and selected MS/MS detection conditions

| Compounds | Retention time (min) | Precursor ion | | Product ion | | | | | |
|--------------|----------------------|---------------|-----------------|--------------|----------------------|-----------------|--------------|----------------------|-----------------|
| | | m/z | Q1 pre-bias (V) | Quantitation | | | Confirmation | | |
| | | | | m/z | Collision energy (V) | Q3 pre-bias (V) | m/z | Collision energy (V) | Q3 pre-bias (V) |
| 12 | 2.53 | 301.1 | 10 | 255.05 | 25 | 11 | 270.9 | 21 | 12 |
| | | | | | | | 79.05 | 40 | 11 |
| Megazol (IS) | 1.97 | 225.3 | 14 | 58 | 23 | 11 | 166.05 | 13 | 16 |

Validation procedure for whole blood

Validation protocol and the set of acceptance criteria were as follows:

- Linearity: Calibration curve was generated by plotting the peak area ratios (analyte/internal standard) vs the expected concentration. Linearity of the calibration curve was evaluated by a quadratic regression analysis using a $1/x^2$ weighting. A value greater than 0.99 was expected for the coefficient of determination (r^2).
- Precision and accuracy of the method were assessed at lower limit of quantitation (LLOQ; 10ng/ml) and at the two quality control concentrations (75 and 625 ng/ml). Precision is calculated as the coefficient of variation (CV%) within a single run (intra-assay; n=5) and between different assays (inter-assay; n=5), and accuracy is the percentage of deviation between nominal and found concentration with the established calibration curve. Acceptance criteria were intra-assay and inter-assay precision (CV%) and an accuracy (bias) less than 20 %.
- The lower limit of quantification (LLOQ) was estimated to be the minimal concentration with accuracy and precision within +/-20%. The lower limit of detection (LLOD) was calculated based on a signal-to-noise ratio >3.

- Extraction recoveries were determined by comparing the LLOQ and the quality controls samples (n=5) with their extracted blank whole blood counterparts spiked at the correct concentration after extraction (n=3). CV% in the extraction recovery had to be less than 20%.
- The effect of dilution was investigated on samples spiked at 5-fold (5,000 ng/ml) and 20-fold (20,000 ng/ml) of ULOQ then re-analyzed after ten- and forty-fold dilutions. Precision CV and bias were set less than 20% to successfully validate.
- The absence of carryover was checked by injecting blank samples just after the analysis of the most concentrated sample (1,000 ng/ml).

2. Experimental spectra (NMR + HRMS) of hit-compounds 7, 12 & 13

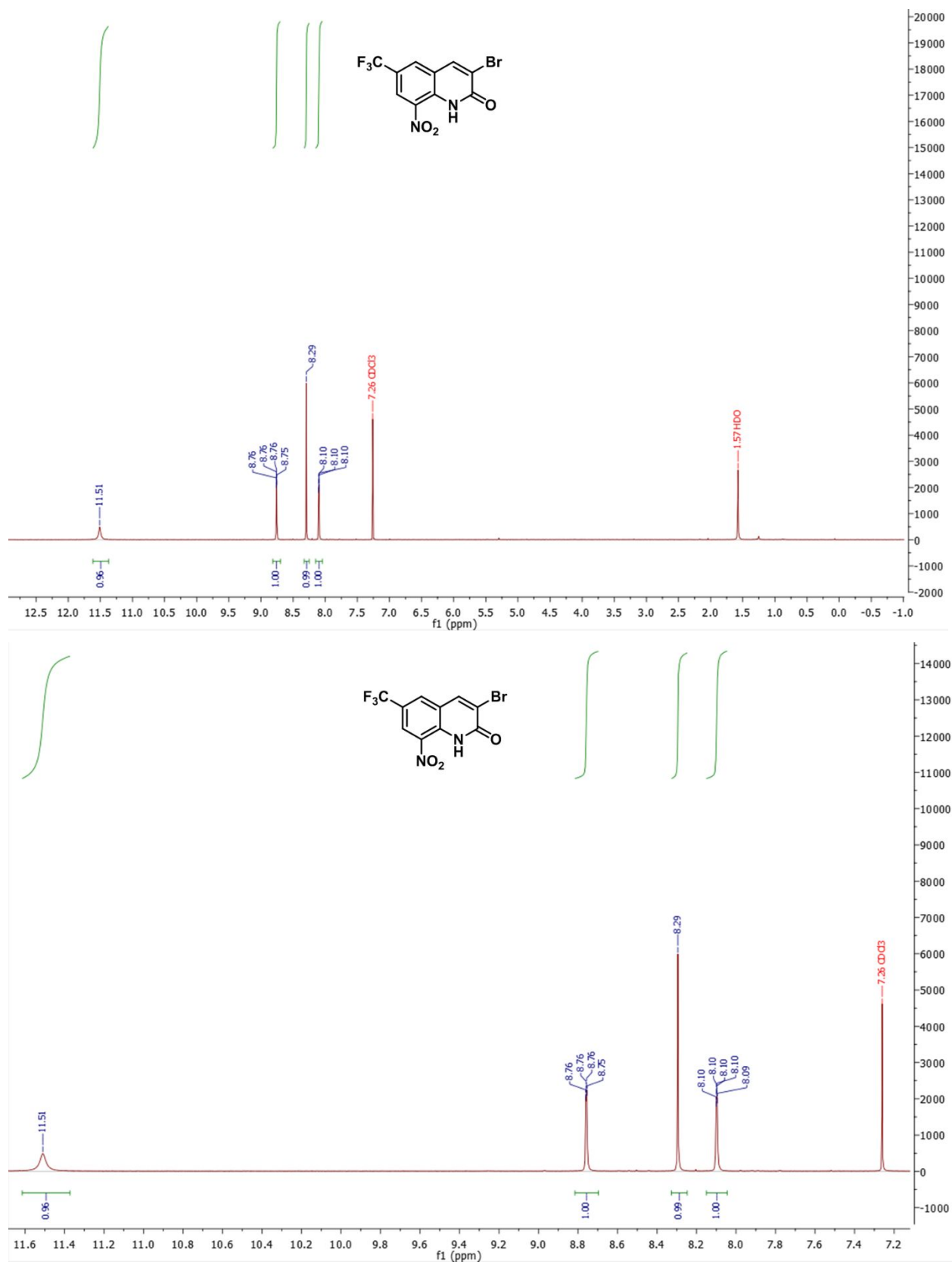


Figure S1: ¹H NMR spectrum of hit compound 7 and zoom between 7.2 and 11.6 ppm.

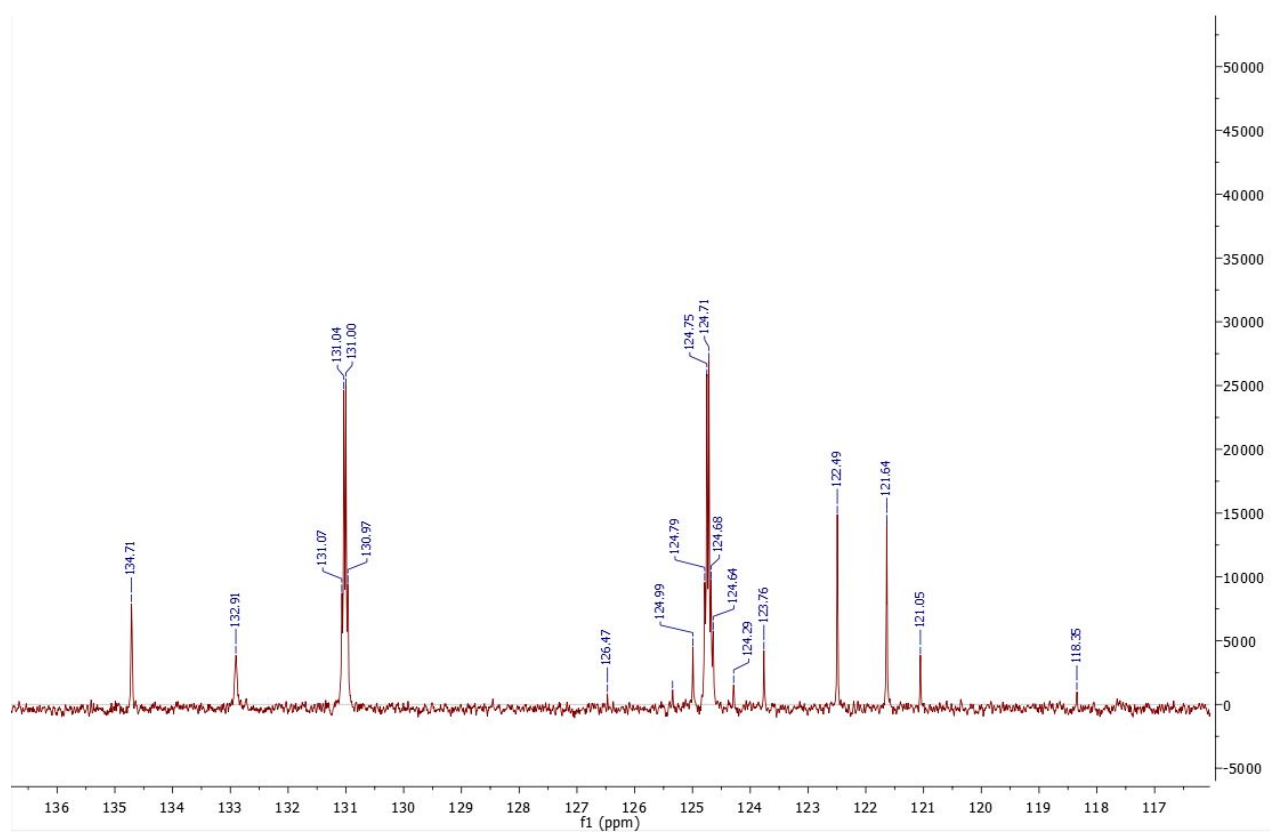
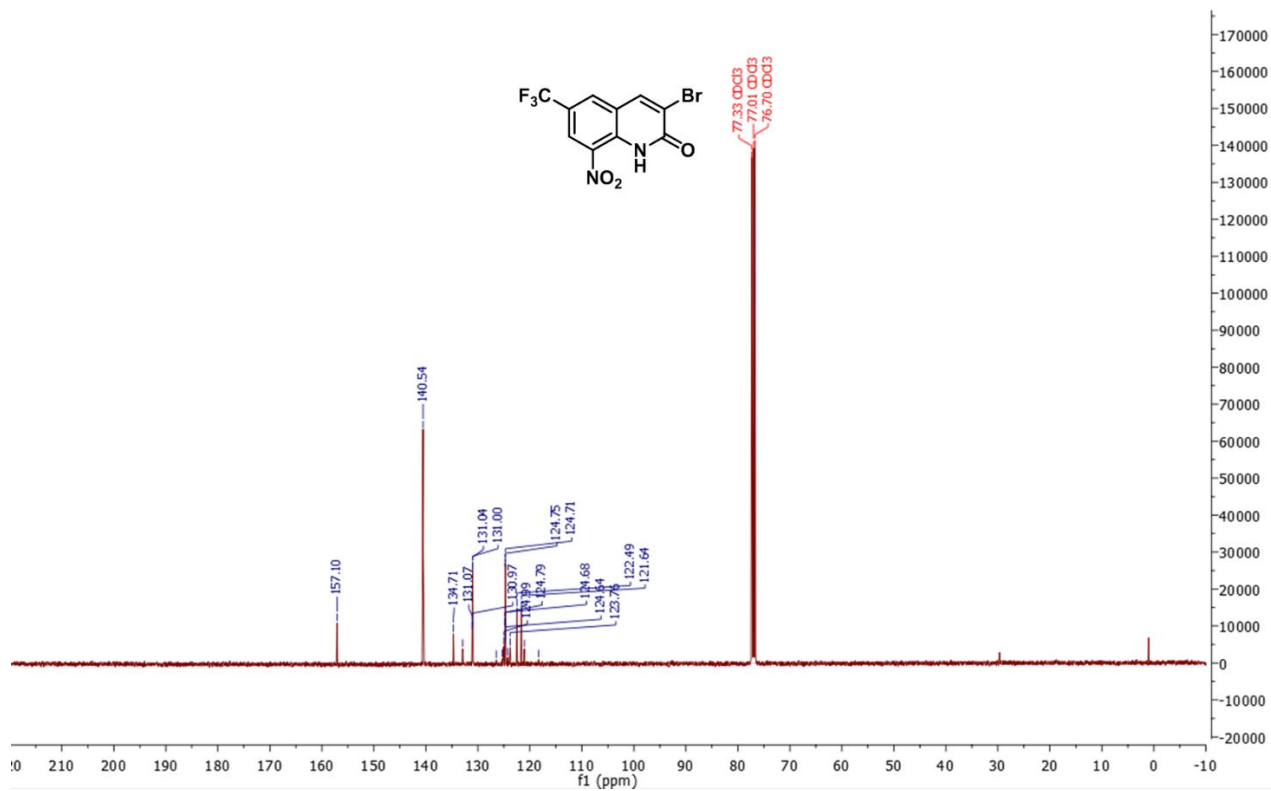


Figure S2: ¹³C NMR spectrum of hit compound 7 and zoom between 117 and 136 ppm.

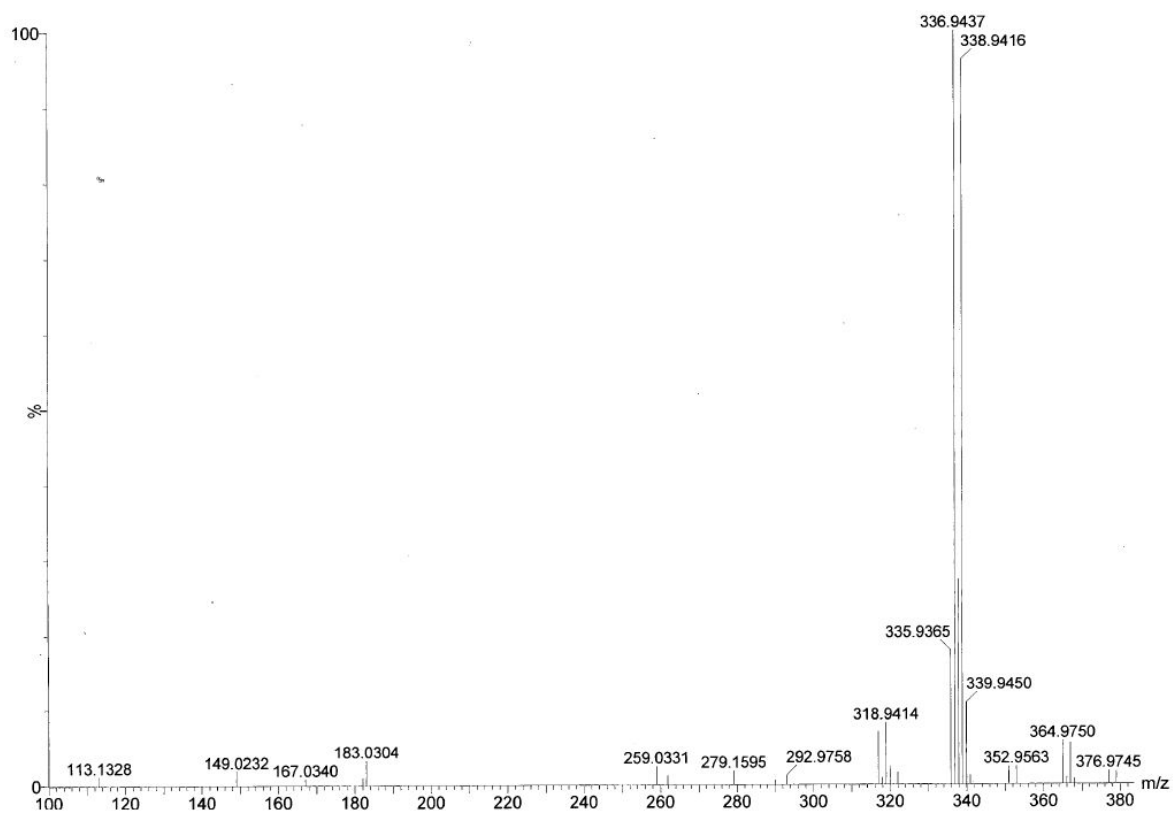


Figure S3: HRMS spectrum of hit compound **7** (DCI CH₄).

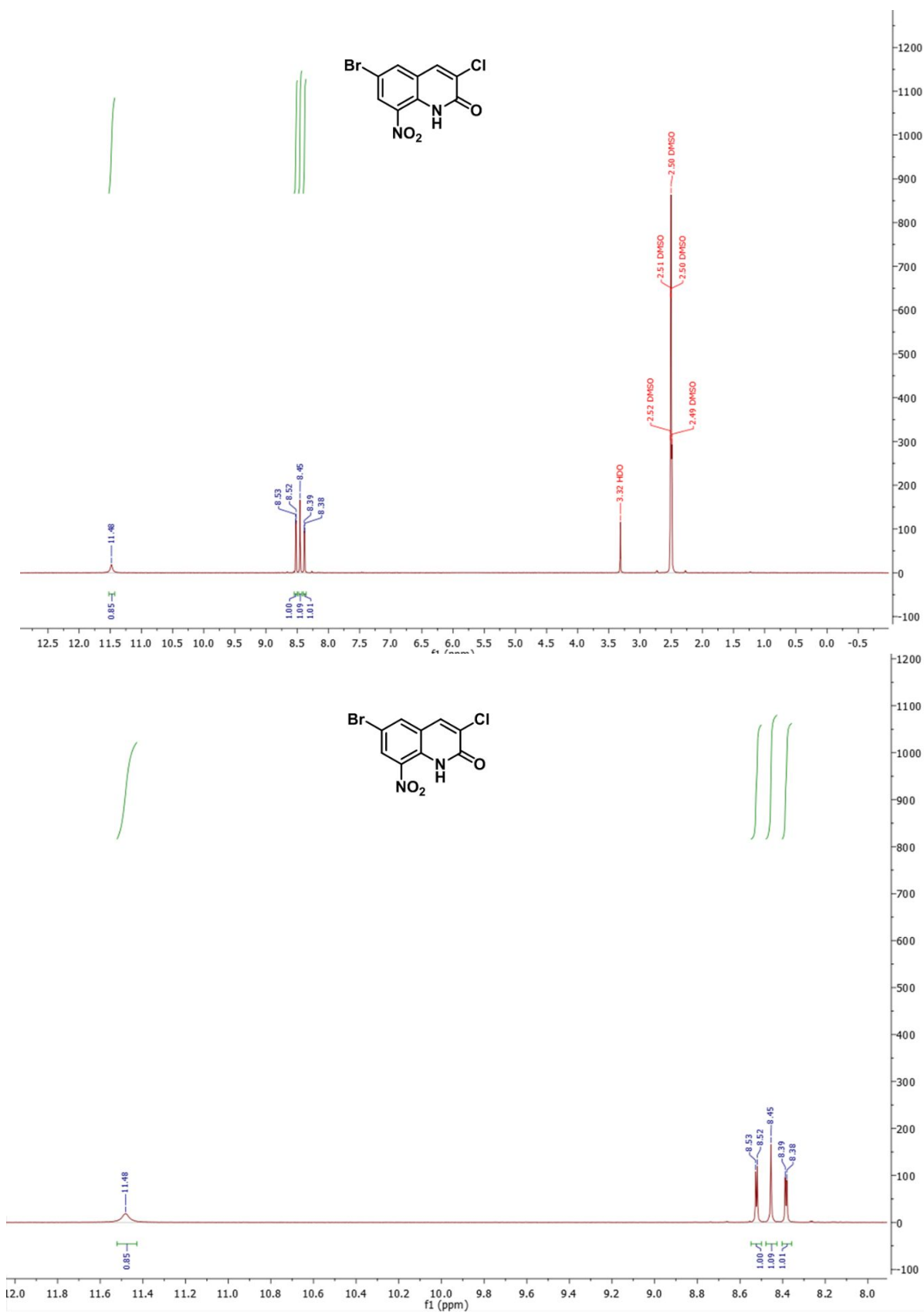


Figure S4: ¹H NMR spectrum of hit compound **12** and zoom between 8.0 and 12.0 ppm.

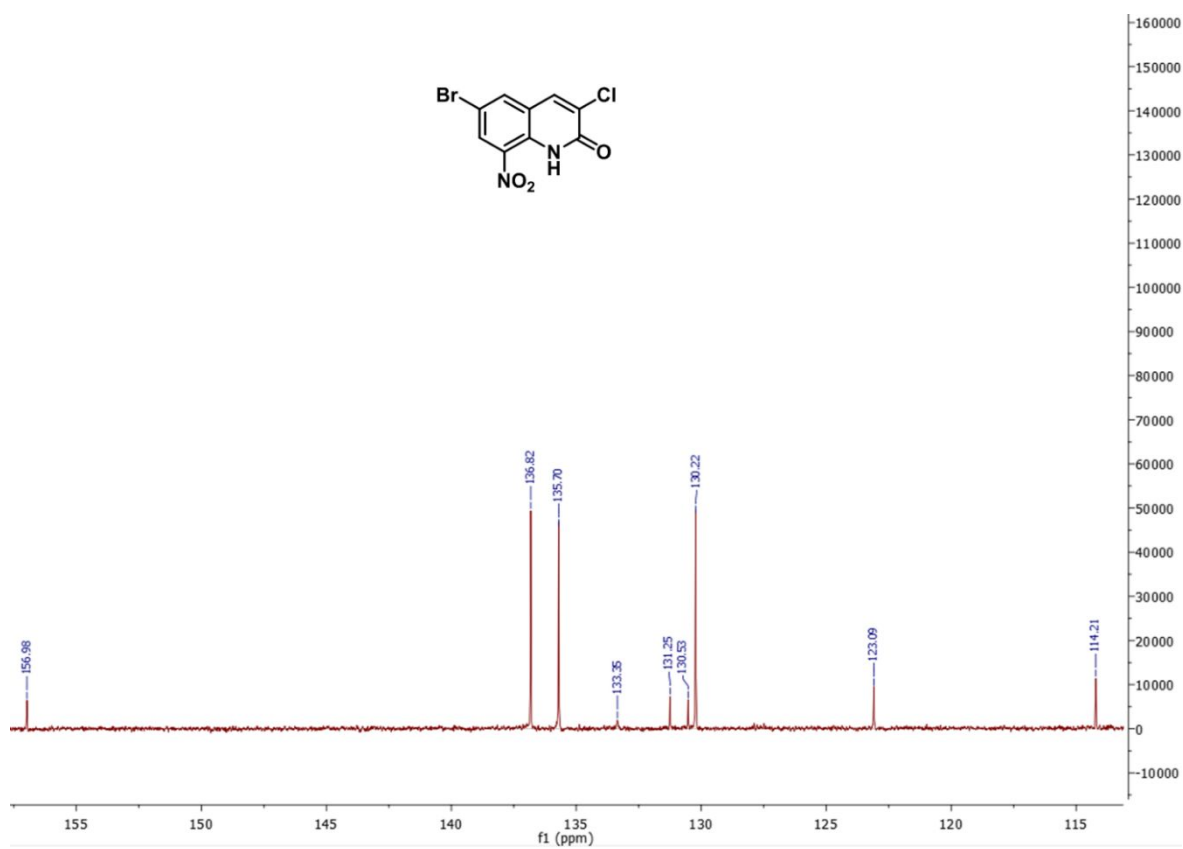
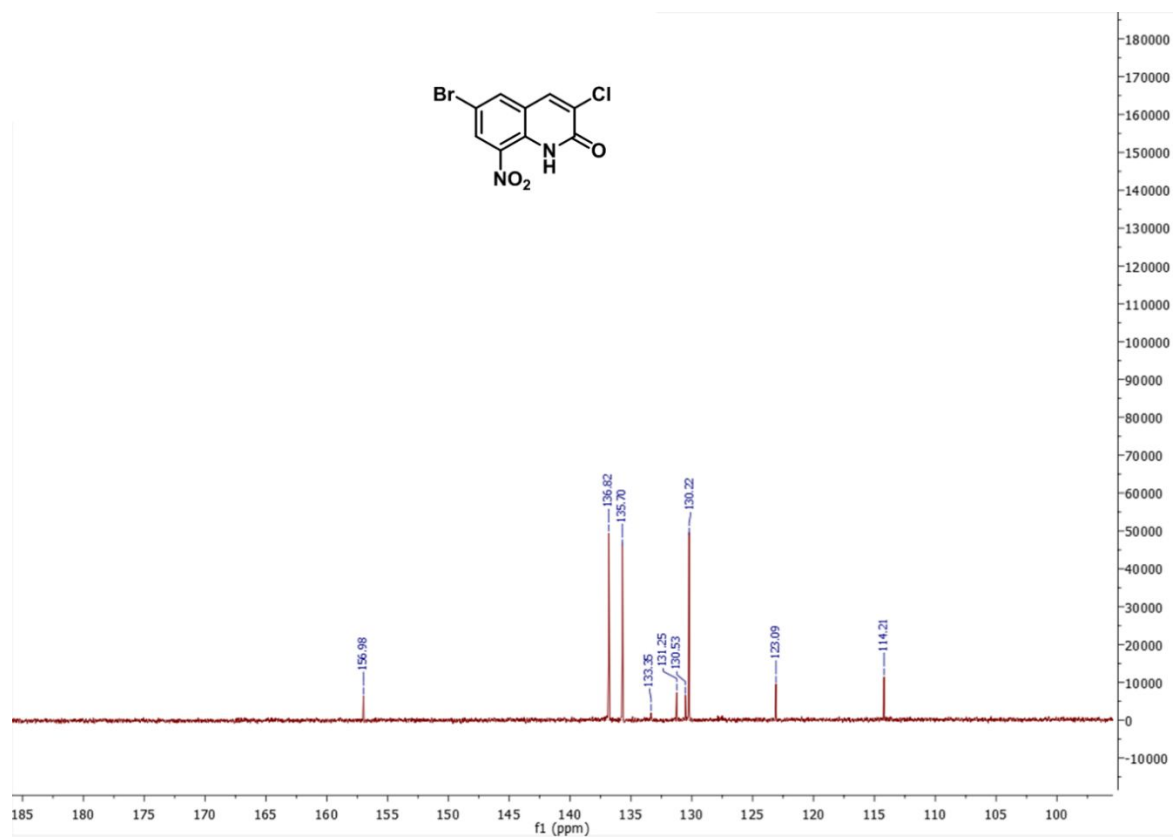


Figure S5: ^{13}C NMR spectrum of hit compound **12** and zoom between 113 and 160 ppm.

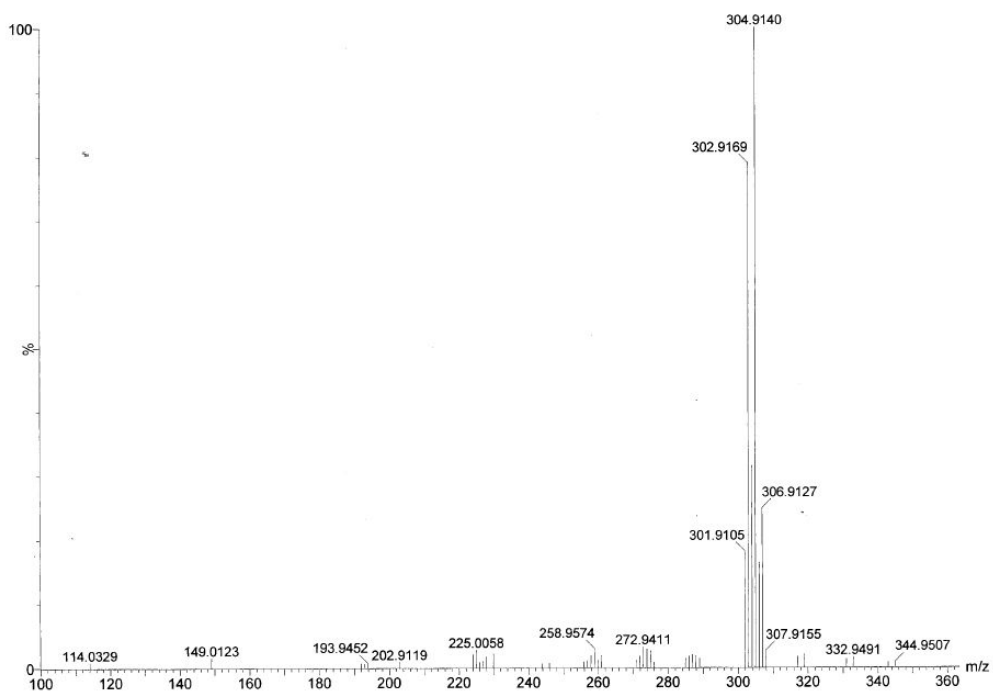


Figure S6: HRMS spectrum of hit compound **12** (DCI CH₄).

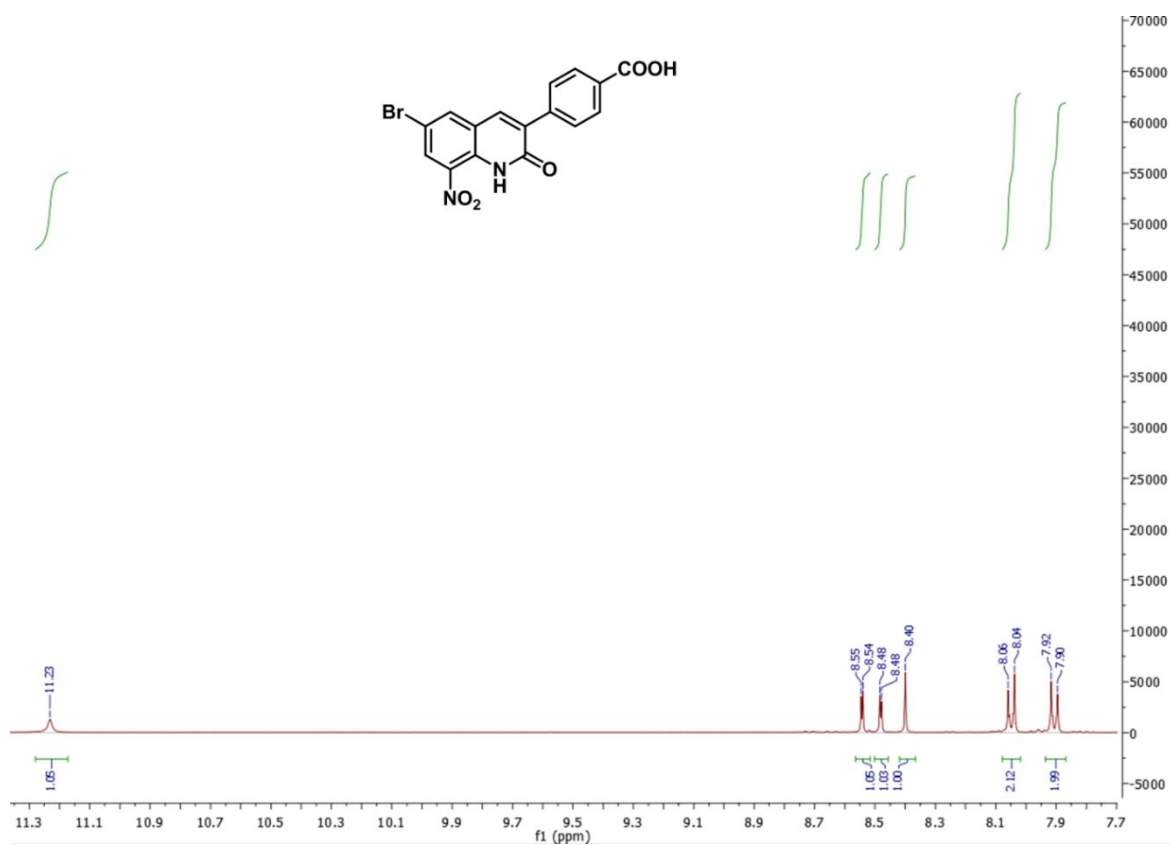
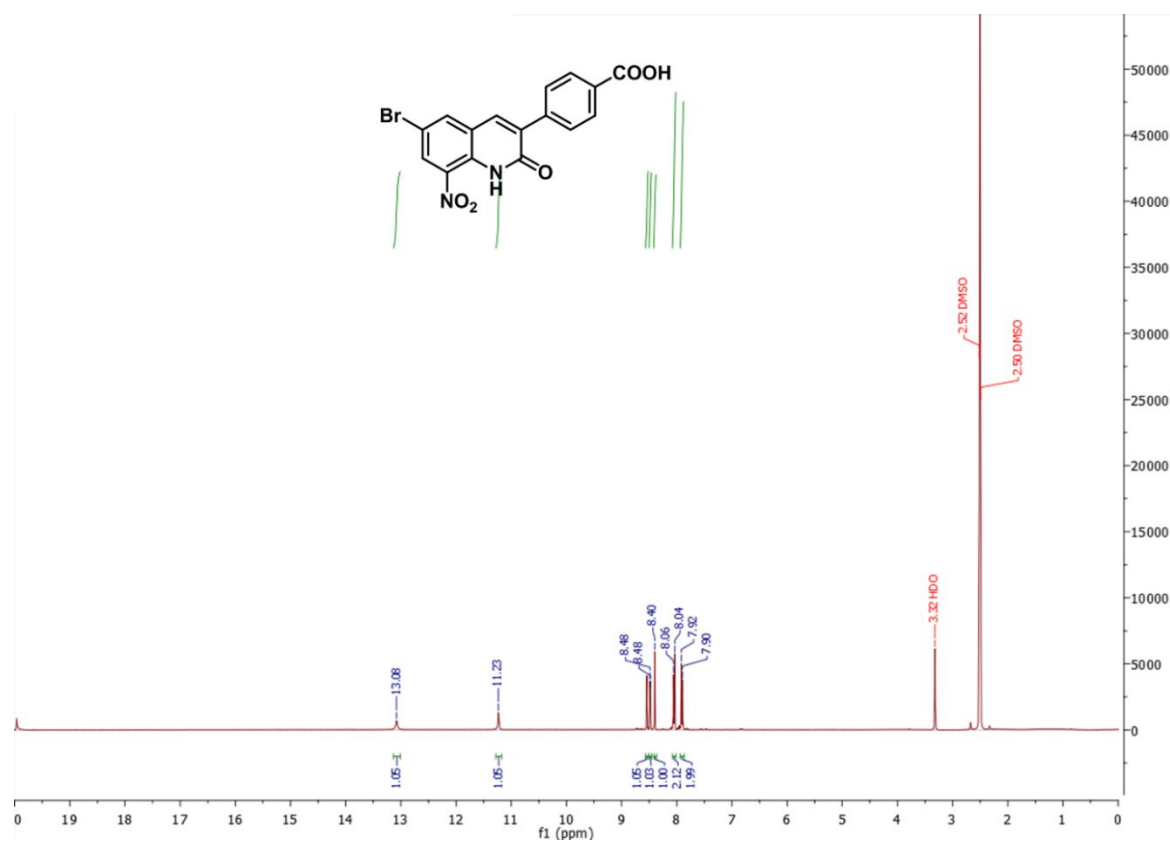


Figure S7: ¹H NMR spectrum of hit compound **13** and zoom between 7.7 and 11.3 ppm.

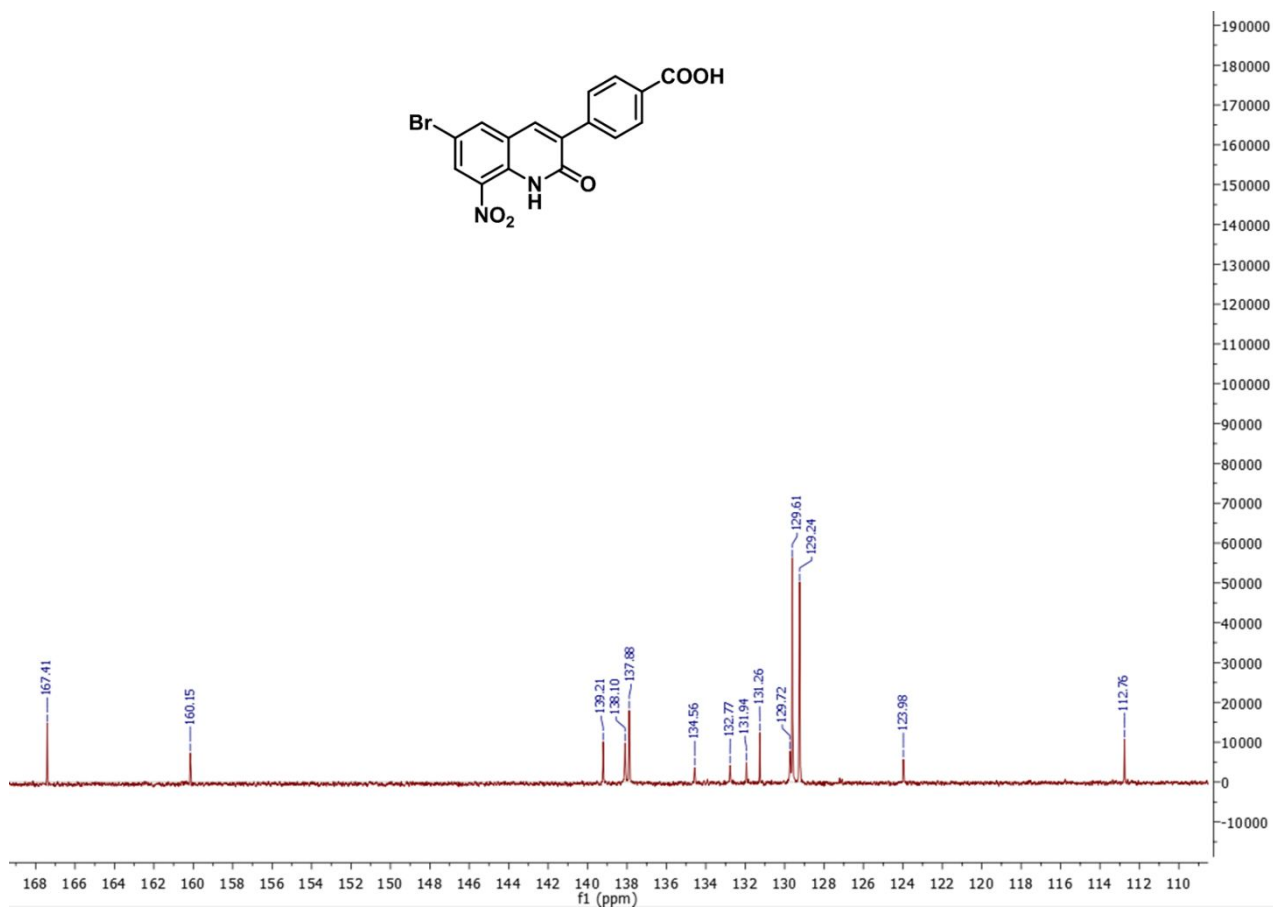
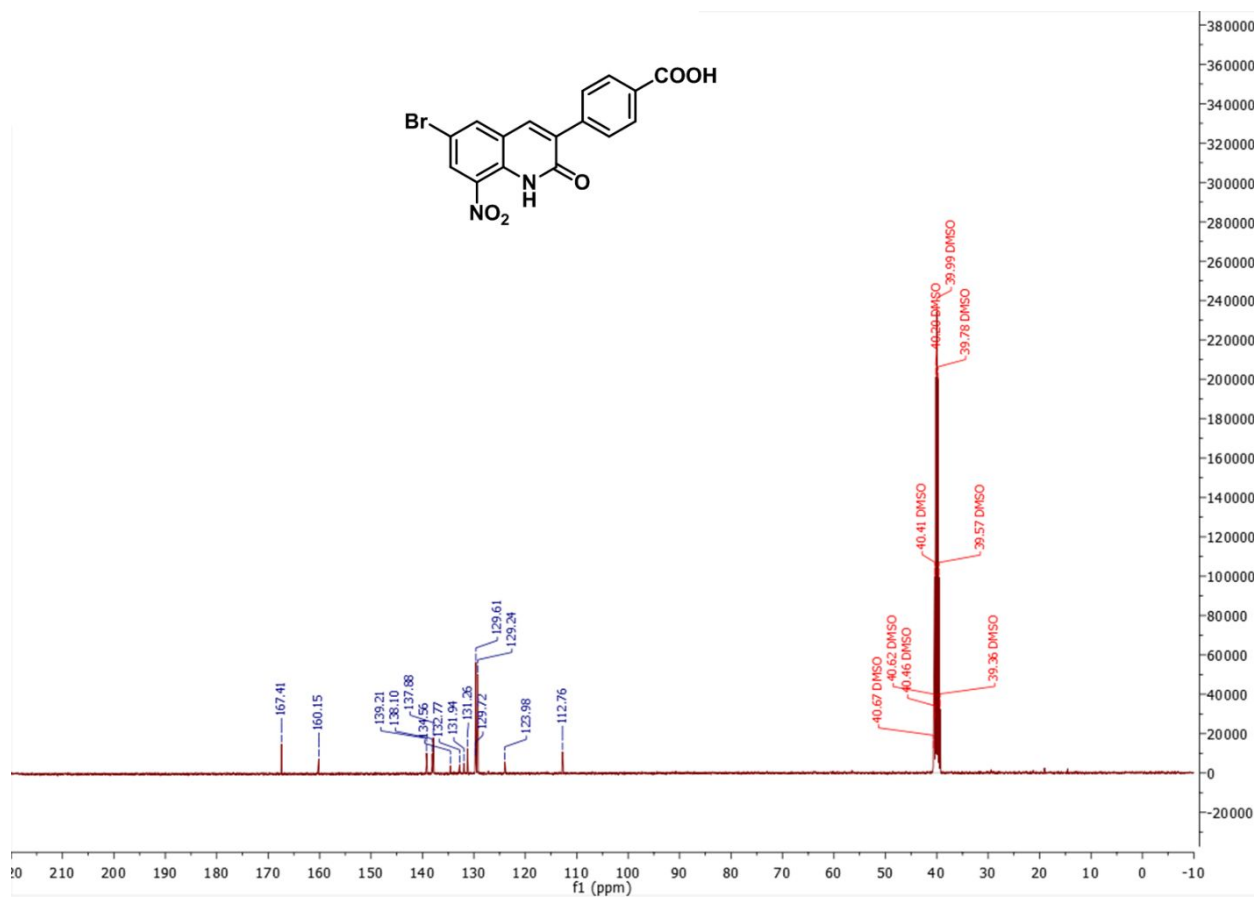


Figure S8: ¹³C NMR spectrum of hit compound **13** and zoom between 110 and 168 ppm.

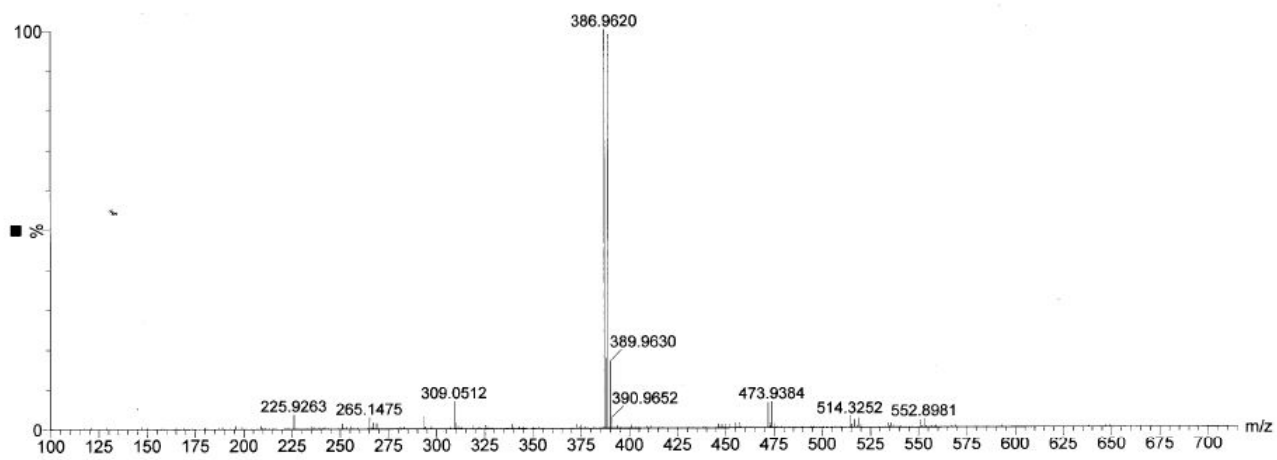


Figure S9: HRMS spectrum of hit compound **13** (ESI -).

3. In vitro pharmacokinetic assays

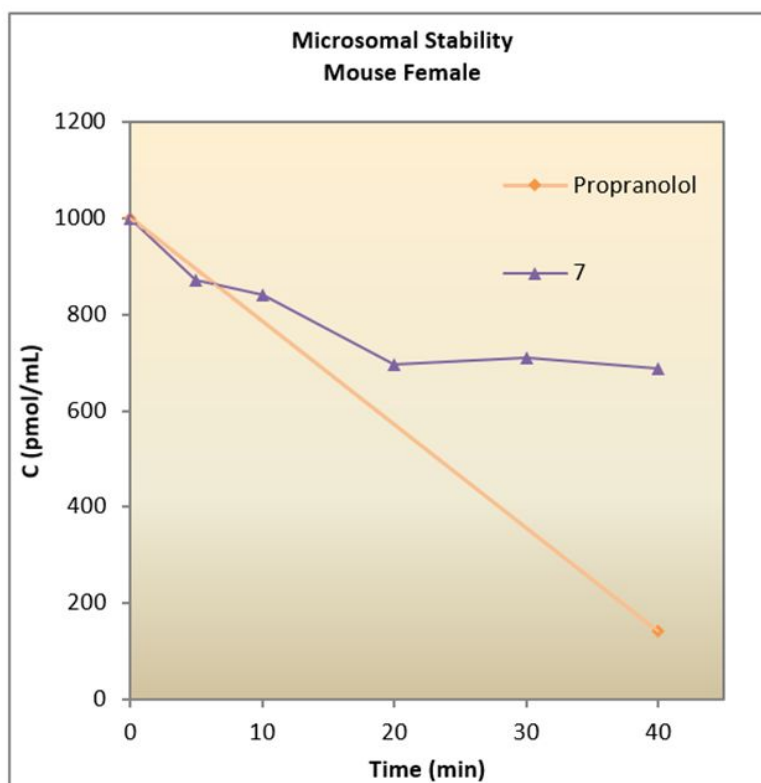


Figure S10: Microsomal stability of hit compound 7.

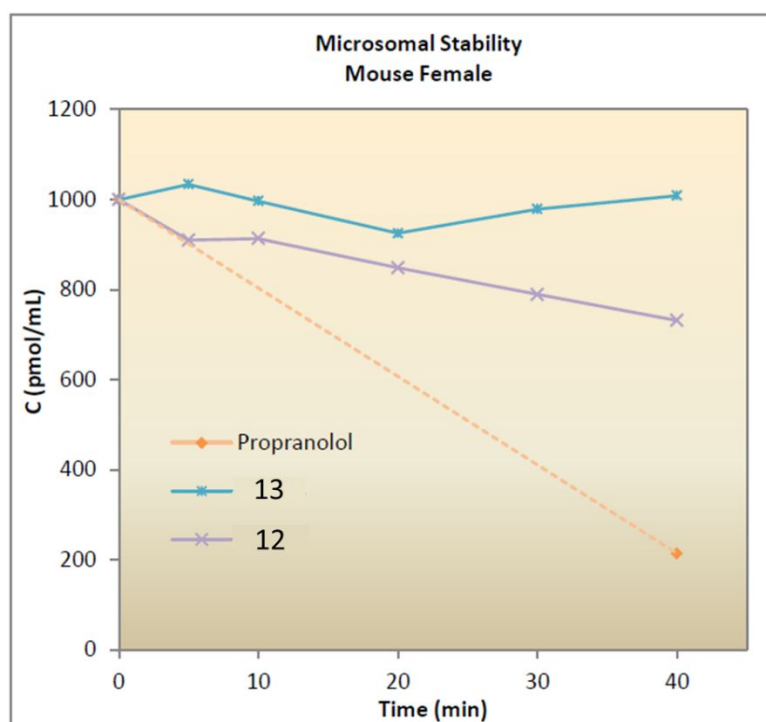


Figure S11: Microsomal stability result of hit compounds 12 and 13.

| Compound ID | Buffer chamber | Plasma chamber | % Bound | | | f _u | | | Log f _u |
|-------------|---------------------------------------|---------------------------------------|---------|---------|------|----------------|---------|--------|--------------------|
| | A _{analyte} /A _{IS} | A _{analyte} /A _{IS} | Value | Average | sd | Value | Average | sd | Value |
| Diclofenac | 0,002 | 0,845 | 99,75 | 99,76 | 0,03 | 0,002 | 0,002 | 0,0003 | -2,614 |
| | 0,002 | 0,856 | 99,79 | | | | | | |
| | 0,002 | 0,870 | 99,73 | | | | | | |
| Warfarin | 0,097 | 11,234 | 99,14 | 99,16 | 0,02 | 0,009 | 0,008 | 0,0002 | -2,074 |
| | 0,096 | 11,518 | 99,17 | | | | | | |
| | 0,093 | 11,098 | 99,16 | | | | | | |
| 7 | 0,000 | 0,041 | 99,13 | 99,44 | 0,28 | 0,009 | 0,006 | 0,0028 | -2,250 |
| | 0,000 | 0,042 | 99,67 | | | | | | |
| | 0,000 | 0,042 | 99,52 | | | | | | |

Figure S12: Plasma protein binding assays of hit compound 7.

| Compound | Buffer chamber | Plasma chamber | % Bound | | | f _u | | | Log f _u |
|------------|---------------------------------------|---------------------------------------|---------|---------|------|----------------|---------|--------|--------------------|
| | A _{analyte} /A _{IS} | A _{analyte} /A _{IS} | Value | Average | sd | Value | Average | sd | Value |
| Warfarin | 0,0860 | 9,3000 | 99,08 | 99,07 | 0,02 | 0,0092 | 0,0093 | 0,0002 | -2,032 |
| | 0,0880 | 9,2760 | 99,05 | | | | | | |
| | 0,0840 | 9,2130 | 99,09 | | | | | | |
| Diclofenac | 0,0010 | 0,6150 | 99,84 | 99,79 | 0,09 | 0,0016 | 0,0021 | 0,0009 | -2,673 |
| | 0,0020 | 0,6320 | 99,68 | | | | | | |
| | 0,0010 | 0,6310 | 99,84 | | | | | | |
| 13 | 0,0000 | 0,0400 | | >99,0 | | | <0,0100 | | <2,000 |
| | 0,0000 | 0,0390 | | | | | | | |
| | 0,0000 | 0,0410 | | | | | | | |
| 12 | 0,0010 | 0,1010 | 99,01 | 99,02 | 0,01 | 0,0099 | 0,0098 | 0,0001 | -2,007 |
| | 0,0010 | 0,1020 | 99,02 | | | | | | |
| | 0,0010 | 0,1020 | 99,02 | | | | | | |

Figure S13: Plasma protein binding assays of hit compounds 12 and 13.

| Compound | Tested concentration | Pe (nm/s) |
|----------------|----------------------|---------------|
| 7 | 100 μM | 450.3 ± 170.5 |
| 12 | 100 μM | 405.1 ± 69.3 |
| 13 | 100 μM | 12.7 ± 0.9 |
| Theophylline | 250 μM | 5.5 ± 0.3 |
| Corticostérone | 100 μM | 138.6 ± 22.0 |

Figure S14: BBB PAMPA assay for hit compounds 7, 12 and 13.

4. Comet assay

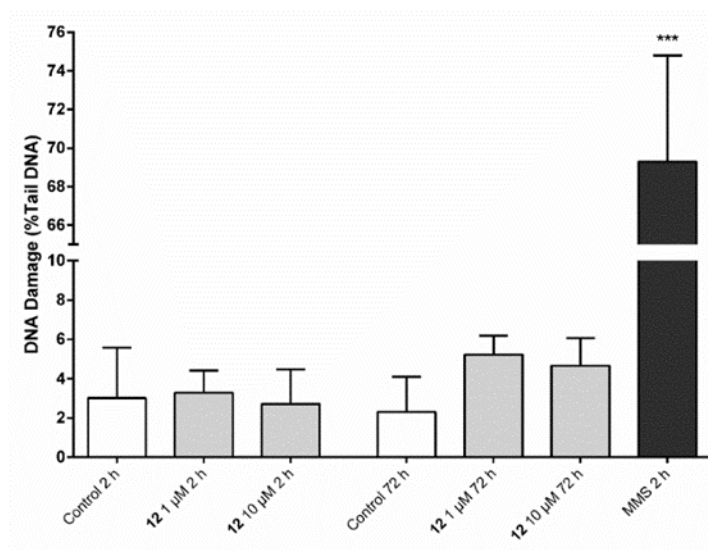


Figure S15. Comet assay on HepG2 cells for compound **12**. Positive control: 1 mM methylmethanesulfonate (MMS). Results are mean \pm SD of three independent experiments. Statistical analysis was performed by one-way ANOVA followed by Dunnett's multiple comparison for each time (***) $P < 0.001$ versus control).

5. In vivo pharmacokinetic study

Following the developed extraction procedure, the preparation of a classical batch that includes 9 calibration standards, 2 internal quality controls, and 20 whole blood samples required less than 1.5 hour. The chromatographic separation of the compound and its internal standard was obtained in 8 min. As presented in Figure S16, acceptance criteria were obtained for both the intra-assay and the inter-assay precision and accuracy. The CV% values in the extraction recovery were also less than 20%. Using quadratic regression with a $1/x^2$ weighting, the coefficients of determination of the calibration curves between 10 and 1,000 ng/ml were higher than 0.99. According to these results, the LLOQ was considered to be 10 ng/ml and the LLOD was determined at 5 ng/ml.

Figure S16: Main parameters of the validation protocol

| | | LLOQ 10 ng/ml | LQC 75 ng/ml | HQC 625 ng/ml | 5*ULOQ 5,000 ng/ml | 20*ULOQ 20,000 ng/ml |
|-----------------------------------------------------|-------------------|------------------|-----------------|------------------|-----------------------|-------------------------|
| <i>Coefficient of determination (r²)</i> | | | | 0.9950 ± 0.0051 | | |
| Recovery (%) (%CV) (n=3) | | 105.4% (17.7%) | 102.1% (2.7%) | 92.7% (5.9%) | | |
| Intra-assay (n=5) | | | | | | |
| | Mean ± SD (ng/ml) | 9.47 ± 1.44 | 79.35 ± 2.11 | 622.04 ± 39.87 | | |
| | Accuracy | 94.7% | 105.8% | 99.5% | | |
| | CV% | 15.2% | 2.7% | 6.4% | | |
| Inter-assay (n=5) | | | | | | |
| | Mean ± SD (ng/ml) | 10.21 ± 0.86 | 76.42 ± 6.41 | 652.54 ± 33.45 | | |
| | Accuracy | 102.1% | 101.9% | 104.4% | | |
| | CV% | 8.4% | 8.4% | 5.1% | | |
| dilution test (n=3) | | | | | | |
| ten-fold dilution | Mean ± SD (ng/ml) | | | | 3,773.3 ± 721.3 | |
| | Accuracy (%CV) | | | | 75.5% (19.1%) | |
| forty-fold dilution | Mean ± SD (ng/ml) | | | | 5,257.1 ± 163.3 | 21,432.4 ± 1,004.0 |
| | Accuracy (%CV) | | | | 105.1% (3.1%) | 107.2% (4.7%) |

Figure S17. Pharmacokinetic parameters of hit compound **12** in whole blood of mouse after oral administration at 25 mg/kg (n = 4)

| | C_{max} (ng/mL) ± SD | T_{max} (h) ± SD | T_{1/2} (h) ± SD | AUC_{0-inf} (ng.h/mL) ± SD | Clairance (mL/h) ± SD |
|-----------|----------------------------------------|------------------------------------|------------------------------------|----------------------------------------------|---------------------------------|
| 12 | 17428 ± 8337 | 1,5 ± 1 | 2,87 ± 0,95 | 123495 ± 31693 | 0,00768 ± 0,0021 |

6. Cyclic voltammograms

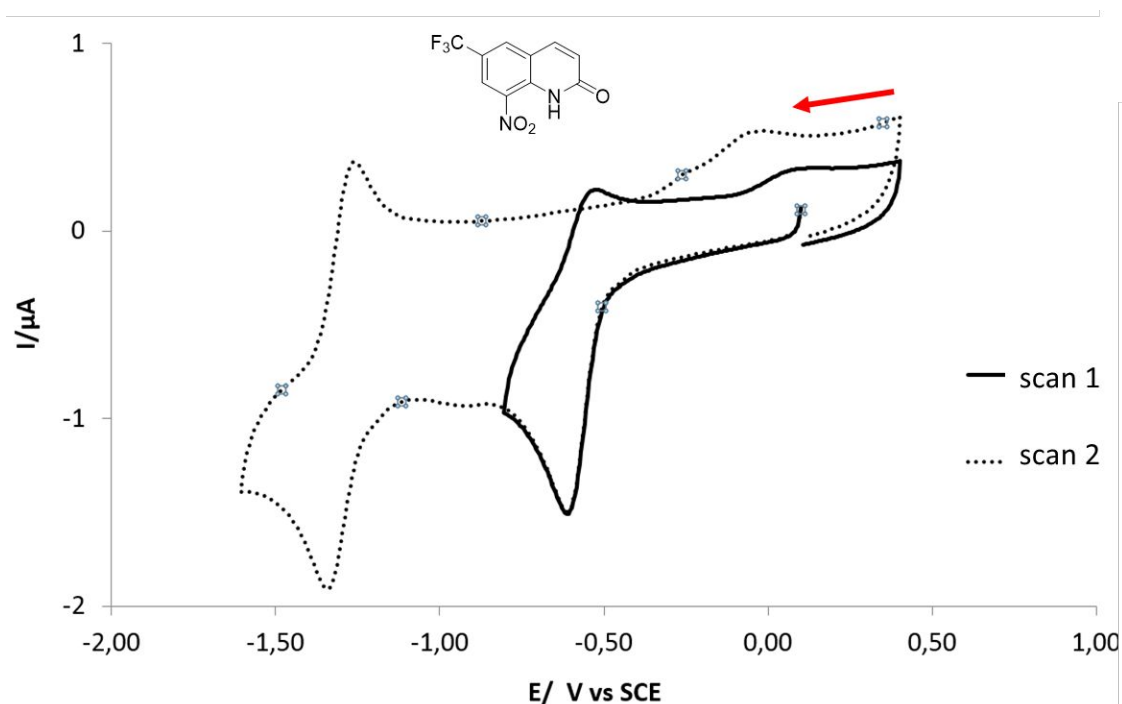


Figure S18: Cyclic voltammetry of compound **7** (10^{-3} mol L⁻¹) in DMSO + 0.1 mol L⁻¹ of (n-Bu₄N)[PF₆] on GC microdisk ($r = 0.5$ mm) at room temperature. Scan rate: 0.2 V s⁻¹.

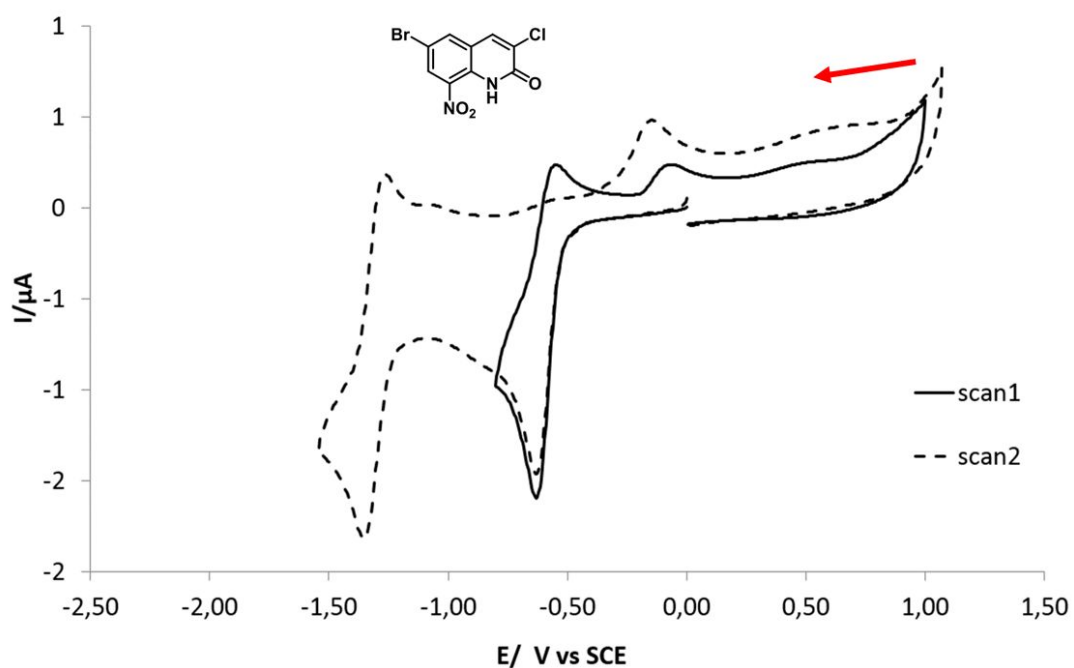


Figure S19: Cyclic voltammetry of compound **12** (10^{-3} mol L⁻¹) in DMSO + 0.1 mol L⁻¹ of (n-Bu₄N)[PF₆] on GC microdisk ($r = 0.5$ mm) at room temperature. Scan rate: 0.2 V s⁻¹.

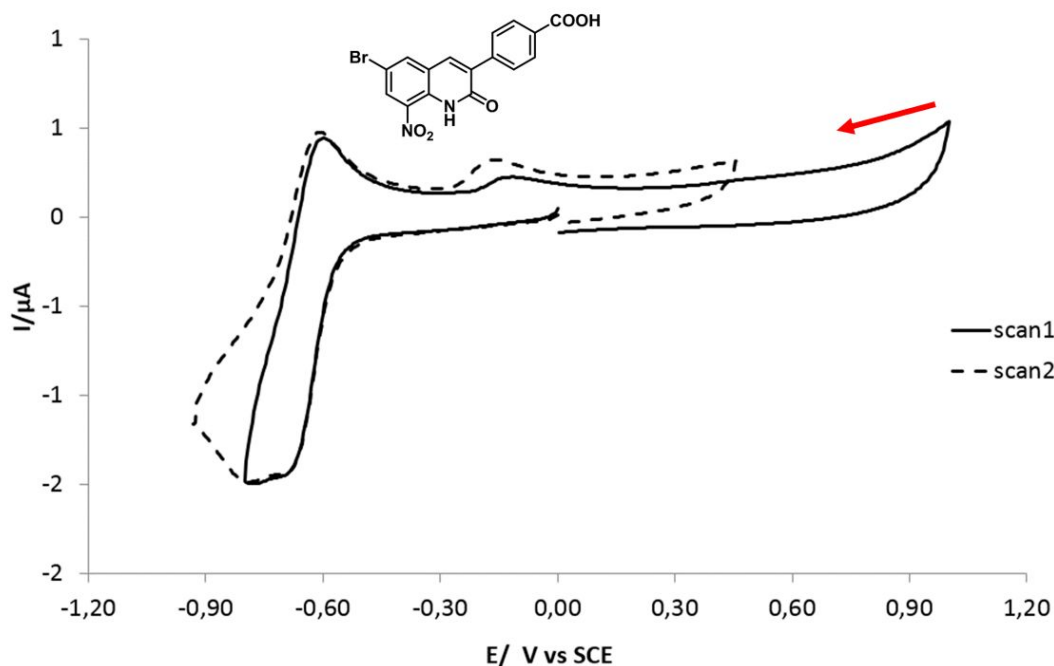


Figure S20: Cyclic voltammetry of compound **13** (10^{-3} mol L $^{-1}$) in DMSO + 0.1 mol L $^{-1}$ of (n-Bu $_4$ N)[PF $_6$] on GC microdisk ($r = 0.5$ mm) at room temperature. Scan rate: 0.2 V s $^{-1}$.

7. REFERENCES

1. Zhang, C., Bourgeade-Delmas, S., Alvarez, A. F., Valentin, A., Hemmert, C., and Gornitzka, H. (2018) Synthesis, characterization, and antileishmanial activity of neutral *N*-heterocyclic carbenes gold(I) complexes. *Eur. J. Med. Chem.* 143, 1635-1643. DOI: 10.1016/j.ejmech.2017.10.060.
2. Goyard, S., Segawa, H., Gordon, J., Showalter, M., Duncan, R., Turco, S.J., and Beverley, S. M. (2003) An *in vitro* system for developmental and genetic studies of *Leishmania donovani* phosphoglycans. *Mol Biochem Parasitol.* 130, 31-42. DOI: 10.1016/S0166-6851(03)00142-7.
3. Wyllie, S., Patterson, S., and Fairlamb, A. H. Assessing the essentiality of leishmania donovani nitroreductase and its role in nitro drug activation. *Antimicrob. Agents Chemother.* **2013**, 57, 901-906.
4. Wyllie, S., Roberts, A. J., Norval, S., Patterson, S., Foth, B. J., Berriman, M., Read, K. D. and Fairlamb, A. H. Activation of bicyclic nitro-drugs by a novel nitroreductase (NTR2) in *Leishmania*. *PLoS Pathog.* 2016, DOI: 10.1371/journal.ppat.1005971.
5. Wyllie, S., Patterson, S., Stojanovski, L., Simeons, F. R. C., Norval, S., Kime, R., Read, K. D., and Fairlamb, A. H. The anti-trypanosome drug fexinidazole shows potential for treating visceral leishmaniasis. *Sci. Transl. Med.* **2012**, 4, 119re1.

6. Baltz, T., Baltz, D., Giroud, C., and Crockett, J. (1985) Cultivation in a semi-defined medium of animal infective forms of *T. brucei*, *T. equiperdum*, *T. evansi*, *T. rhodesiense* and *T. gambiense*. *EMBO J.* 4, 1273-1277.
7. Rätz, B., Iten, M., Grether-Bühler, Y., and Kaminsky, R. (1997) The AlamarBlue® Blue assay to determine drug sensitive of African trypanosome (*T. brucei rhodesiense* and *T. brucei gambiense*) *in vitro*, *Acta Trop.* 68, 139-147. DOI: 10.1016/S0001-706X(97)00079-X.
8. Guillon, J., Cohen, A., Das, R. N., Boudot, C., Gueddouda, N., Moreau, S., Ronga, L., Savrimoutou, S., Basmaciyan, L., Tisnerat, C., Mestanier, S., Rubio, S., Amaziane, S., Dassonville-Klimpt, A., Azas, N., Courtioux, B., Mergny, J-L. Mullié, C., and Sonnet, P. (2018) Design, synthesis, and antiprotozoal evaluation of new 2,9-bis[(substituted-aminomethyl)phenyl]-1,10-phenanthroline derivatives. *Chem. Biol. Drug Des.* 91, 974-995. DOI: 10.1111/cbdd.13164.
9. Greig, N., Wyllie, S., and Patterson, S, and Fairlamb, A. H. (2009) A comparative study of methylglyoxal metabolism in trypanosomatids. *FEBS J.* 276, 376-86. DOI: 10.1111/j.1742-4658.2008.06788.x.
10. Wyllie, S., Foth, B. J., Kelner, A., Sokolova, A. Y., Berriman, M., and Fairlamb, A. H. (2016) Nitroheterocyclic drug resistance mechanisms in *Trypanosoma brucei*. *J. Antimicrob. Chemother.* 71, 625-34. DOI: 10.1093/jac/dkv376.
11. Jones, D.C., Hallyburton, I., Stojanovski, L., Read, K. D., Frearson, J. A. and Fairlamb, A. H. (2010) Identification of a *kappa*-opioid agonist as a potent and selective lead for drug development against human African trypanosomiasis. *Biochem. Pharmacol.* 80, 1478-86. DOI: 10.1016/j.bcp.2010.07.038.
12. Mosman, T. J. (1983) Rapid colorimetric assay for cellular growth and survival: application to proliferation and cytotoxicity assays. *J. Immunol. Meth.* 65, 55-63, DOI: 10.1016/0022-1759(83)90303-4.
13. Perdry, H., Gutzkow, K. B., Chevalier, M., Huc, L., Brunborg, G., and Boutet-Robinet, E. (2018) Validation of Gelbond® high-throughput alkaline and Fpg-modified comet assay using a linear mixed model, *Environ. Mol. Mutagen.* 59, 595-602, DOI: 10.1002/em.22204.
14. Jourdan, J. P., Since, M., El Kihel, L., Lecoutey, C., Corvaisier, S., Legay, R., Sopkova-de Oliveira Santos, J., Cresteil, T., Malzert-Fréon, A., Rochais, C. and Dallemagne P. (2017)

Benzylphenylpyrrolizinones with anti-amyloid and radical scavenging effects, potentially useful in Alzheimer's disease treatment. *ChemMedChem* 12, 913–916. DOI: 10.1002/cmdc.201700102.

15. Kerns, D. L., Bezar, I. F., Petusky, S. L. and Huang, Y. (2009) Comparison of blood-brain barrier permeability assays: in situ brain perfusion, MDR1-MDCKII and PAMPA-BBB. *J. Pharm. Sci.* 98, 1980-1991. DOI : 10.1002/jps.21580.

16. Lecoutey, C., Hedou, D., Freret, T., Giannoni, P., Gaven, F., Since, M., Bouet, V., Ballandonne, C., Corvaisier, S., Malzert Fréon, A., Mignani, S., Cresteil, T., Boulouard, M., Claeysen, S., Rochais C. and Dallemagne, P. (2004) Design of donecopride, a dual serotonin subtype 4 receptor agonist/acetylcholinesterase inhibitor with potential interest for Alzheimer's disease treatment. *Proc. Natl. Acad. Sci. USA* 111, E3825-E3830. DOI: 10.1073/pnas.1410315111.

17. Westland, J., Dorman, F., QuEChERS extraction of benzodiazepines in biological matrices (2013) *J. Pharm. Anal.* 3, 509-517. DOI: 10.1016/j.jpha.2013.04.004.

18. Dulaurent S., El Balkhi, S., Poncelet, L., Gaulier J. M., Marquet, P., Saint-Marcoux, F. QuEChERS sample preparation prior to LC-MS/MS determination of opiates, amphetamines, and cocaine metabolites in whole blood (2016) *Anal. Bioanal. Chem.* 408, 1467-1474. DOI: 10.1007/s00216-015-9248-3.